THE EFFECTS OF ENERGY DENSITY ON THE MECHANICAL PROPERTIES OF SS316L PRODUCED BY SELECTIVE LASER MELTING

NUR AQILAH BINTI DERAHMAN

DEPARTMENT OF MECHANICAL
FACULTY OF ENGINEERING
UNIVERSITY OF MALAYA
KUALA LUMPUR

SEPTEMBER 2018

THE EFFECTS OF ENERGY DENSITY ON THE MECHANICAL PROPERTIES OF SS316L PRODUCED BY SELECTIVE LASER MELTING

NUR AQILAH BINTI DERAHMAN

DISSERTATION SUBMITTED IN FULFILMENT OF THE REQUIREMENTS FOR THE DEGREE OF MASTER OF ENGINEERING SCIENCE

DEPARTMENT OF MECHANICAL
FACULTY OF ENGINEERING
UNIVERSITY OF MALAYA
KUALA LUMPUR

SEPTEMBER 2018

UNIVERSITY OF MALAYA

ORIGINAL LITERARY WORK DECLARATION

Name of Candidate: Nur Aqilah Binti Derahman

Matric No: KGA150065

Name of Degree: Master of Engineering Science

Title of Project Paper/Research Report/Dissertation/Thesis ("this Work"):

Investigation into The Effects of Parameters on The Properties of Part Produced by Selective Laser Melting

Field of Study: Advanced Manufacturing Technology

I do solemnly and sincerely declare that:

(1) I am the sole author/writer of this Work;
(2) This Work is original;
(3) Any use of any work in which copyright exists was done by way of fair dealing and for permitted purposes and any excerpt or extract from, or reference to or reproduction of any copyright work has been disclosed expressly and sufficiently and the title of the Work and its authorship have been acknowledged in this Work;
(4) I do not have any actual knowledge nor do I ought reasonably to know that the making of this work constitutes an infringement of any copyright work;
(5) I hereby assign all and every rights in the copyright to this Work to the University of Malaya ("UM"), who henceforth shall be owner of the copyright in this Work and that any reproduction or use in any form or by any means whatsoever is prohibited without the written consent of UM having been first had and obtained;
(6) I am fully aware that if in the course of making this Work I have infringed any copyright whether intentionally or otherwise, I may be subject to legal action or any other action as may be determined by UM.

Candidate's Signature Date:

Subscribed and solemnly declared before,

Witness's Signature Date:

Name:

Designation:

ABSTRACT

Selective laser melting (SLM) is an additive manufacturing (AM) method of fabricating different types of complex components using a layer-by-layer approach. The parts are produced directly from 3D computer-aided design (CAD) data by melting the powdered material layer-by-layer assisted by laser power. In this work, an experimental investigation was conducted into the SLM method process parameters using stainless steel 316L powder. The energy density which are the influence of laser power, scanning speed and hatching distance on the physic-mechanical properties such as surface roughness, dimensional accuracy, tensile strength, and hardness of the manufactured parts were investigated. The design of experiments was conducted using Taguchi's L_{16} orthogonal array. Furthermore, statistical analysis with signal-to-noise response and analysis of variance were applied to obtain the optimal SLM parameter combinations. The experimental results indicated that laser power has the greatest effect on surface roughness, dimensional accuracy and hardness. However, scanning speed exhibited the greatest influence on the tensile strength of manufactured parts, followed by laser power and hatching distance. Next, the optimal parameters obtained were used in regression analysis to predict the mechanical properties. Subsequently, a confirmation experiment was carried out by using the optimal parameters determined. The confirmation experiment results were then compared with the predicted values during experiment validation. Lastly, the shot peening technique was used to improve the quality of the manufactured parts. Based on the results, shot peening improved the quality of the manufactured parts by about 33.28% for surface roughness, 58.33% for dimensional accuracy and 34.24% for hardness.

Keywords: Selective Laser Melting, Additive Manufacturing, Taguchi

ABSTRAK

Pemilihan laser selektif (SLM) adalah kaedah pembuatan tambahan (AM) yang digunakan untuk menghasilkan pelbagai jenis komponen kompleks dengan menggunakan pendekatan lapisan demi lapisan. Bahagian-bahagian itu dihasilkan secara langsung dari data reka bentuk komputer (CAD) 3D, dengan mencairkan bahan serbuk dari satu lapisan demi lapisan dengan bantuan laser. Dalam kerja ini, siasatan eksperimen mengenai parameter proses bagi mesin SLM dengan menggunakan serbuk keluli tahan karat 316L telah dijalankan. Pengaruh kuasa laser, kelajuan pengimbasan dan jarak penetasan terhadap sifat-sifat mekanik bahan yang dihasilkan telah disiasat. Reka bentuk percubaan dijalankan dengan menggunakan susunan ortogon L_{16} Taguchi. Tambahan pula, analisis statistik menggunakan respon isyarat-pada-bunyi dan analisis varians digunakan untuk mendapatkan kombinasi parameter yang optimum bagi proses SLM. Dari hasil penyiasatan, didapati bahawa kuasa laser mempunyai kesan terbesar pada kekasaran permukaan, ketepatan dimensi dan kekerasan berbanding kelajuan pengimbasan dan jarak penetasan. Walau bagaimanapun, kelajuan pengimbasan merupakan pengaruh terbesar pada kekuatan tegangan bahan diikuti dengan kuasa laser dan kemudian jarak penetasan. Seterusnya, analisis regresi telah dijalankan untuk meramalkan nilai sifat mekanik dengan menggunakan parameter optimum yang diperolehi. Selanjutnya, eksperimen pengesahan dilakukan dengan menggunakan parameter optimum yang diperolehi bagi setiap penemuan. Hasil daripada itu dibandingkan dengan nilai yang diramalkan. Akhir sekali, teknik pukulan digunakan untuk meningkatkan kualiti bahan. Berdasarkan hasilnya, proses ini dapat meningkatkan kualiti bahagian pembuatan sekitar 33.28% dalam kekasaran permukaan, 58.33% dalam ketepatan dimensi dan 34.24% dalam kekerasan.

Kata Kunci: Pemilihan Laser Selektif, Pembuatan Tambahan, Taguchi

ACKNOWLEDGEMENTS

First and foremost, I would like to convey my deepest gratitude to Allah SWT for giving me strength and patience to complete this research study despite the many difficulties experienced in the process of experimenting and also writing the dissertation. Without His consent, I would not have any of this.

I am deeply indebted to my project supervisor Dr. Mohd Sayuti Bin Ab. Karim from the University of Malaya, Kuala Lumpur, who has assisted, guided and encouraged me throughout all my research and dissertation writing. He has guided me in this project with essential theoretical information, especially on the rapid prototyping process. My supervisor's mentorship has been tremendously helpful in completing this research.

I greatly appreciate Contraves Advanced Devices Sdn. Bhd. for allowing me to prepare the samples at the facility with the necessary manpower, equipment and data support. Without these, this research study would not have been possible. I would also like to express my gratitude to the technicians at the Faculty of Engineering, UM, for assisting me in many ways to complete the experiments.

Last but not least, thanks to my family members for loving me and pushing me to succeed. Dad, thank you for supporting me the whole time and Mom, thank you for all your efforts towards my education. I will never forget your help and I cannot imagine this life without you.

TABLE OF CONTENTS

LIST OF FIGURES

LIST OF TABLES

LIST OF SYMBOLS AND ABBREVIATIONS

SLM	Selective laser melting
AM	Additive manufacturing
CAD	Computer aided design
SS316L	Stainless steel 316L
E_d, J/mm^2	Energy density, J/mm^2
P, W	Laser Power, Watt
v, mm/s	Scanning speed, mm/s
h_d, mm	Hatching distance, mm
R_a	Average of a set of individual measurements of a surfaces peaks and valleys
UTS	Ultimate tensile strength
HV	Hardness Vickers
S/N	Signal to noise ratio
ANOVA	Analysis of variance
DF	Degree of freedom
ADJ MS	Adjusted mean squares measure
ADJ SS	Adjusted sums of squares
F-Value	Test statistic used to determine whether the term is associated with the response
P-Value	Probability that measures the evidence against the null hypothesis.
R^2	Percentage to determine how close the data with the regression line

CHAPTER 1 : INTRODUCTION

1.1 Background

The manufacturing industry seeking towards improvement on the production from time to time while reducing cost. Nowadays, additive manufacturing (AM) is a technology that can enhance the production process. One of an AM technology is the selective laser melting (SLM), which significantly benefits product design and development. It simplifies the process of the conventional molding method. The process requires minimal setup and lead time to produce the part as well as variance selection of materials. Owing to these special advantages, these technologies have been developing fast since the early 1990s.

The SLM process entails a layer-by-layer approach to produce the final parts by depositing and melting the metallic powder material. Laser is used to melt the metal powder and create the final parts directly from the 3D CAD data. It was invented in 1979 by R.F. Housholder (Stwora & Skrabalak, 2013). The Housholder's initial notion of sintering powder included the movement of a focused heat source on the powder surface, followed by the deposition and consolidation of powder layers with the help of a laser system to melt and join the powder materials in the melt pool.

Some of the factors in laser melting are needed to be considered such as the powder material properties, geometry of the parts and processing parameters. Normally, these factors are influenced by the energy delivered to the powder surface. The physic-mechanical properties of the manufactured parts, e.g. surface roughness, dimensional accuracy, tensile strength, hardness and etc. depends on the energy applied, which is related to the process parameters. A key factor in controlling the quality of the final part is to control the process parameters.

The densification of iron-based powders that was dependent on the processing parameters, such as laser power, layer thickness, scan rate and hatch distance was investigated by (A Simchi, 2006). Besides that, the quality of the physic-mechanical and microstructural properties of the manufactured part depends on the process parameters applied such as building direction, layer thickness and scanning speed (Kruth et al., 2010).

Furthermore, some of the previous research works have mentioned that the shot peening process are recommended in improving the surface quality of the SLM manufactured parts (Calignano, Manfredi, Ambrosio, Iuliano, & Fino, 2012). It is known as a cold working process that is used as a post-processing technique for metallic parts. The objective of this process is to prevent fatigue and corrosion, thereby the life cycle of manufactured parts can be increased. It involves the use of small spherical shots, which are bombarded onto the surface of the manufactured part in other to obtain a better surface finish. The shot peening method has proven to be the most economical and effective way of producing surface residual compressive stresses, thereby increasing the life span of the treated metals.

The focus of this research is to study the influence of varying SLM process parameters, including the laser power, scanning speed and hatching distance on the physic-mechanical properties of manufactured parts.

1.2 Objectives

1. To investigate the effects of processing parameter variations on the physic-mechanical properties of manufactured parts.
2. To optimize the process parameters in order to improve the properties of manufactured parts (surface roughness, dimensional accuracy, strength and hardness).
3. To investigate the effects of the shot-peening process on the surface roughness, dimensional accuracy and hardness of the manufactured part.

1.3 Problem Statement

In this research, the focus is on SLM process parameter matters. Although SLM technology can yield excellent benefits, the sintered part quality is still not good enough to produce accurate and dense parts. Some problems may arise during a very short melting process time due to the high thermal energy required to promote material rearrangement and densification. In order to achieve better quality of built parts, optimized process conditions should be attained by changing the laser power intensity, scan rate and hatch distance. Different process parameters affect the melting quality and ultimately, the quality of parts. Enhancements in manufactured part quality are always desirable in the industry. Much research work remains to be done to improve the performance of rapid prototyping. Furthermore, stainless steel 316L is one of the attractive metallic materials for biomedical applications due to its mechanical properties, biocompatibility, and corrosion resistance but, there's minimal research study in this material by using SLM process.

1.4 Significance of The Study

Selective laser melting (SLM) has recently experienced a rapid rise in usage due to the ability to fabricate complex designs. Although SLM technology is greatly beneficial, the manufactured part quality is still not sufficiently good to produce accurate and dense parts. The quality of manufactured parts depends on the parameters applied during the melting process. Hence, to ensure the quality of manufactured parts is as same as solid materials produced using traditional methods, the optimum parameters are determined in this study.

1.5 Scope of The Study

This study focuses on the physic-mechanical properties of stainless steel 316L manufactured part by using SLM machine with different setting parameters. Process parameters involved in this study are laser power, scanning speed and hatching distance. Also, this study is limited to design of experiments by Taguchi Method with L_{16} orthogonal array (OA) and three control parameters with four levels each.

1.6 Organization of The Dissertation

This dissertation consists of five chapters as follows:

Chapter one provides a general overview of selective laser melting and a problem statement that is addressed in this study. It also includes the scope of the research as well as the study goals and objectives.

Chapter two presents the literature review, which summarizes literature and sources including journals, books and periodicals from the previous researchers. The theory related to the study and previous outcomes are discussed in this chapter.

In chapter three, the material selection employed for the sample model in this research project is discussed. The design of experiment used to conduct the experiments is also

presented. Moreover, the chapter gives a detailed description of the project methodology including the suitable parameters and setup utilized to conduct the mechanical testing.

Chapter four consists of the results and discussion of this research project. The results are presented in tables prior to analysis. The collected data are analyzed using MINITAB software and explained in graphical form.

Chapter five concludes the major findings that are in agreement or disagreement with the study objectives. Finally, recommendations are made for further improvement in future works.

CHAPTER 2 : LITERATURE REVIEW

2.1 Background

The manufacturing industry is always seeking ways to improve production processes by reducing the product processing costs, reducing the time consumption to fabricate complex parts, etc. Additive manufacturing (AM) is the best approach to solve the difficulties encountered when fabricating complex parts or using difficult materials by conventional manufacturing techniques. The AM process can directly produce functional prototypes and tools with no post-processing procedures. Rapid prototyping (RP) is an additive manufacturing process that can help to improve the production process by applying layers upon layers to produce parts. This advanced manufacturing technology was first commercialized in the mid-1980s (Delgado, Ciurana, & Rodríguez, 2011). SLM is a RP technology that facilitates the direct fabrication of prototypes or assembly models using 3D computer-aided design (CAD) databases without tools or fixtures and without producing any big material waste such as scrap (Calignano et al., 2012).

Achieving the desired surface quality is very important for the functional behaviour of a part. The quality of a part that is manufactured by SLM does not only depend on the surface roughness aspect, but it is the keys in fulfilling the part manufacturing requirements during the process. In recent years, the surface quality of SLM parts has posed major drawbacks, whereby the surface roughness of manufactured parts is still high in comparison to solid materials achieved by conventional methods (Badrossamay & Childs, 2006; Kruth et al., 2010). On the other hand, the process-dependent nature of the surface roughness formation mechanism along with numerous uncontrollable factors that influence pertinent phenomena, make it almost impossible to find a straightforward solution. The most common strategy

involves in selecting conservative process parameters, neither guarantee the achievement of the desired surface finish nor attain high metal removal rates (Benardos & Vosniakos, 2003).

According to (Delgado et al., 2011), the process parameters need to be controlled to attain better dimensional accuracy. The dimensional accuracy of parts manufactured through the Shrinkage during the SLM process is another significant factor that determines the dimensional accuracy of manufactured parts. Shrinkage can take place when the substrate temperature is in a crucial stage (Chung & Das, 2006).

The main parameters involved in this process are the laser power, scanning speed, hatching distance, layer thickness, building direction, working atmosphere and powder bed temperature. Hence, it is necessary to study the parameters to ensure the quality of the parts manufactured by SLM is comparable with the parts manufactured using conventional method.

2.3 Selective Laser Melting Process

In the manufacturing industry, parts manufacturers and end users are always searching for design alternatives. With an SLM machine it is possible to fabricate highly complex, tailored and fully formed parts with minimal time consumption. Only a single step is required to produce solid parts using this technology without the need for part-specific tooling.

SLM has the capability producing fully dense parts without post-processing process. It only needs to remove the manufactured part and supports from base plate. By producing manufactured part that have low porosity and high strength, SLM is more superior compared to SLS in AM. Normally, post-processing process such as material infiltration and heat treatment are needed to improve the quality of the SLS manufactured part. Also, post-processing requires more time and significantly lengthens the lead time. Full melting of

powder is achieved in SLM because of the use of high-intensity laser and binder materials without the post-processing processes. SLM technology provides improvements in production lead time, quality of the product, and reliability of the manufactured part compared to binder-based laser sintering AM processes (Yap et al., 2015).

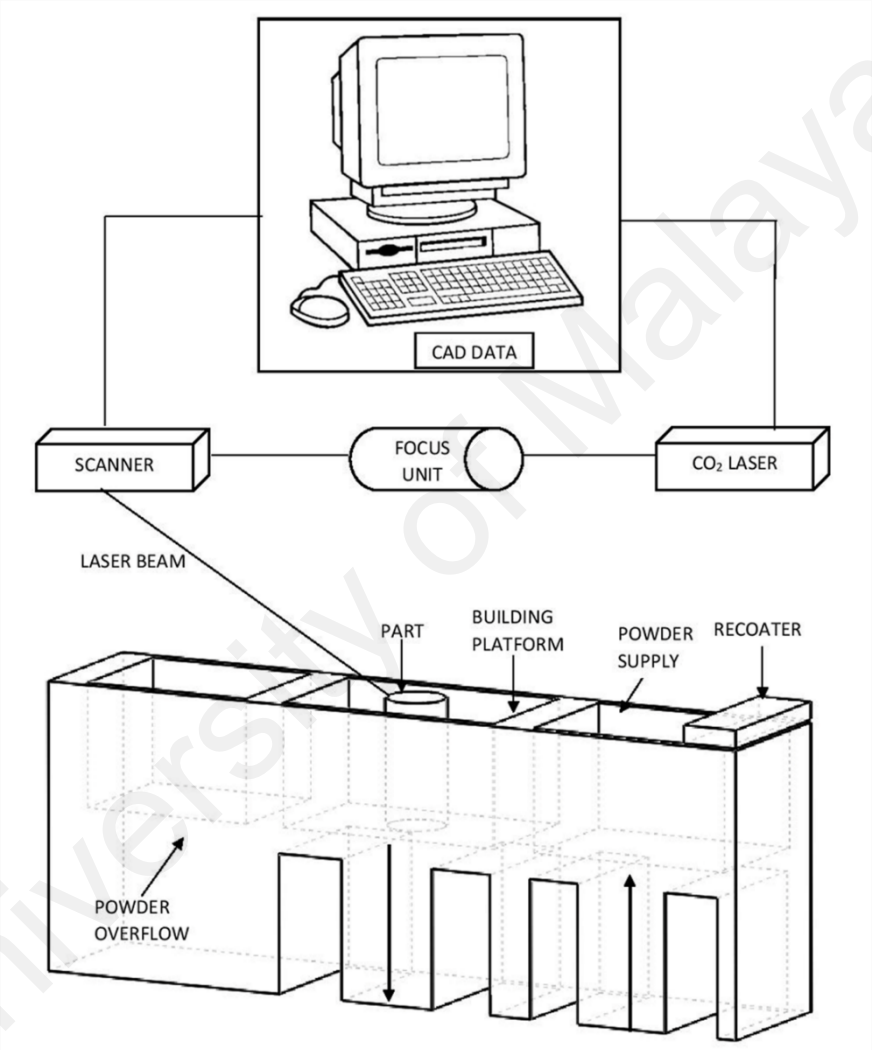

Figure 2.1: Basic of SLM process

According to the SLM process shown in Figure 2.1, the CAD data transfers the design directly to the machine to fabricate a part via the layer-by-layer with the aid of high laser power. High laser power helps to fuse small powder particles together. One layer of powder is spread over the building platform and heated just below the melting temperature. With the

help of the laser, the temperature will slightly increase and selectively melt the powder particles. The building platform is lowered by one-layer thickness upon the completion of one layer. Subsequently, a new material layer is applied on top of the melted layer. When the laser is exposed to the new layer, it melts and bonds to the previous layer. The process is repeated until the object is completed. The solid part is built up through the consolidation of powder particles with a focused laser beam that selectively scans the powder bed surface. It occurs either by diffusion bonding or actual fusion of the powder particles (Calignano et al., 2012).

The basic components of this technology normally comprise a laser system including an optical system, a recoater for spreading the powder on the powder bed, feed pistons to store the fresh powder, and a cylinder where the part is manufactured. Other components included may be heaters located above the feed pistons. A computer controls all these components through separate programmable logic controllers, electronics and sensors (Stucker, 2001).

In addition, the process can mesh layers above/onto each other at one time to create more objects. Excess powder can be reused, but it still needs to be thoroughly sieved before the next usage.

2.4 Materials

Laser melting is utilized to build parts of metallic materials that are fully melted. Several materials can be used with this technology, such as low-cost powders like tool, brass and steel, or high-quality materials like Inconel, titanium, nitinol and cobalt chrome. Stainless steel 316L is known as one of the metallic materials that provide better mechanical properties, corrosion resistance and biocompatibility (Dewidar, Khalil, & Lim, 2007). Also, this material is popular metal for use in biomedical such as acetabula cup (one half of an artificial hip joint) applications. Current applications of stainless steel 316L processed by SLM have been

studied in (Tolosa, Garciandía, Zubiri, Zapirain, & Esnaola, 2010) to produce dental caps; ultralight structures with over 450 holes and channels per cubic meter for aircraft, automotive, and medical industries; thin walled (0.5 mm) 40×40-mm assembly parts; and chirurgical devices. This popularity stems from a satisfactory combination of good mechanical properties and reasonable cost.

2.5 Process Parameters

Several input parameters need to be controlled or varied since the final quality of the manufactured parts totally depends on the SLM process parameters applied. The SLM process parameters are shown in Figure 2.2:

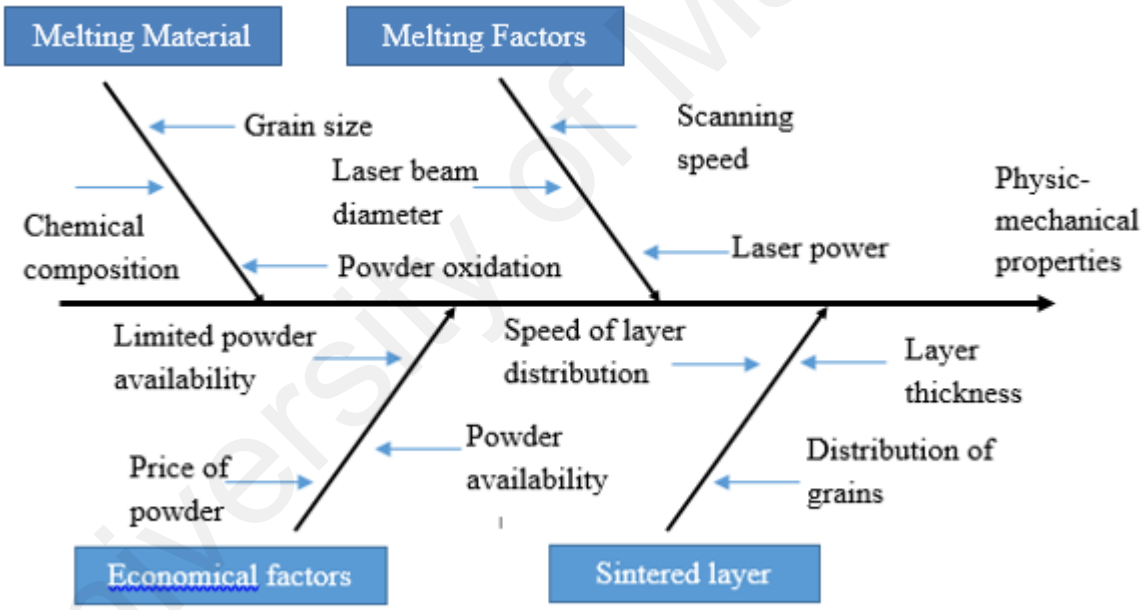

Figure 2.2: SLM process parameters (Stwora & Skrabalak, 2013)

The quality of manufactured parts are also affected by some parameters that impact the energy density (Krishnan et al., 2014). Energy density is given in Equation (2.1):

$$E_d = \frac{P}{v \,.\, h_d} \qquad (2.1)$$

Where, E_d = Energy density (J/mm^2) P = laser power (W), h_d = hatching distance (mm) and v = scanning speed (mm/s).

The energy density is also computed from the nominal values of the process parameters by using Equation (2.1). Based on Equation (2.1), high laser power and/or low scanning speed will increase the energy density and temperature. Then the energy density must be increased to produce metal parts, but greater energy density may produce curling effects. The thermal effect of the laser energy raises the bed temperature, so the loose powder will bond together (A. Simchi & Pohl, 2003).

2.5.1 Laser Power

Laser power contributes significantly to the surface quality of manufactured parts. Lower laser power produces lower surface roughness results. In contrast, applying higher laser power can smoothen and improve the melt pool in the layer connection and increase the wettability of the melt. Hence, high laser power reduces the occurrence of the balling phenomenon by relieving surface tension variations. Moreover, large amounts of material can vaporize when the laser power is too high, which disrupts the melt pool surface and increases the top surface roughness (Calignano et al., 2012).

Defects like shrinkage, warping and balling may develop when unsuitable laser power values are applied. High laser power could completely melt and even break up the material due to excessive shrinkage and high residual stresses, producing many visible cracks (Zhang, Liao, & Coddet, 2012). However, insufficient energy from low laser power might not induce significant melting of the metallic powders, which would inevitably lead to laminated structure formation in the powders.

Laser power has a significant effect on the density, because when greater laser power is applied, it leads to higher densification (Stwora & Skrabalak, 2013). This is in line with the energy density calculated, whereby with increasing laser power the energy density also increases (Krishnan et al., 2014; A. Simchi & Pohl, 2003).

Laser power has an important influence on hardness, because hardness has a direct relationship with the densification level. Hardness decreases when lower laser power is applied. This is due to the many un-melted particles and the balling phenomenon that occurs. Low laser power only melts the surface resulting a poor bond neck between the particulates. This indicates that the parts have no mechanical strength and present a loose metal structure (Zhang et al., 2012).

The effect of laser power on the parts manufactured with material by SLM on the dynamic mechanical properties was studied by (Sharma, Singh, Sachdeva, & Kumar, 2013). They found that the surrounding powder particles as well as the target particles melted as the powder bed received an extra heat when the laser power was increased to higher levels. Furthermore, high laser power had delivered extra energy to the powder material for sintering and melting. Hence, the powder particles became closely packed, which boosts mechanical properties.

The effects of laser power on the tensile properties and structure of printing materials in parts manufactured with titanium(Ti) powder were studied by (Hanzl, Zetek, Bakša, & Kroupa, 2015). The researchers found that the energy transferred to the powder influenced the melting temperature as well as the liquid phase extent in the melted components. Laser power was the main parameter affecting the mentioned energy. Based on the microstructural analysis in Figure 2.3, high laser power formed a fully consistent melted surface. However, a porous structure with open pores at the surface was exhibited when the laser power was reduced.

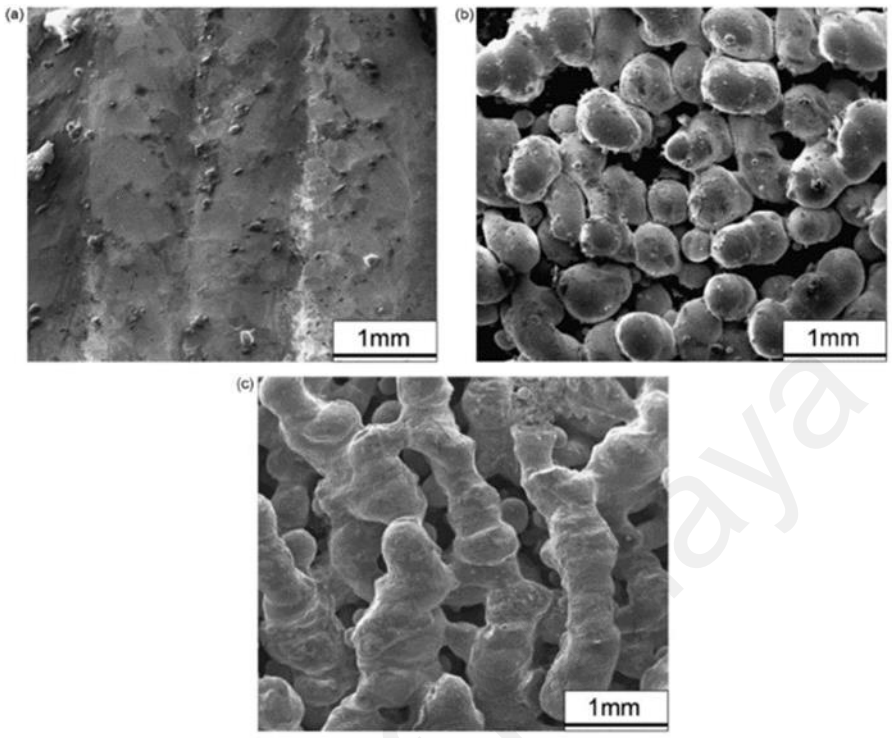

Figure 2.3: Structure of samples: a) fully consistent surface, b) surface with balling phenomenon, c) porous structure

Meanwhile, (Negi, Dhiman, & Sharma, 2015) asserted that raising the laser power from low to high levels raises the mechanical properties, such as the yield strength and ultimate tensile strength. The reason is that, high energy input was transferred to the material to ensure it melted properly when the laser power was increased. Thus, when a closely packed model was generated, it will increase the strength of the parts. Furthermore, by increasing the laser power, the temperature of the melt increases, which increases the cooling rate and leads to reduction of grain size.

2.5.2 Scanning Speed

Scanning speed is one of the most substantial parameters that need to be controlled when producing prototypes using SLM. Previous researchers have stated that the quality of a manufactured part depends on the scanning speed applied. The production rate can be improved by increasing the scanning speed, but this will cause greater energy density that

affects the manufactured part properties. (Y.-A. Song & Koenig, 1997) reported that reducing the scanning speed will widen the scan lines and hence, decreased the porosity percentage.

Scanning speed has the greatest influence on surface roughness (Calignano et al., 2012). Low scanning speed results in better surface finish, since the melt pools have more time to smoothen before solidification. However, the volume amount of liquid formed within the melt pool may increase when the scanning speed applied is too low. This is because of the same melt pool may widen, causing a higher thermal difference over it and thus leading to greater surface tension variations. Then the melt pool may break off into smaller entities – a process known as "balling" that increases the surface roughness.

Hardness of the manufactured part will be increased when the scanning speed increased. This can be attributed to the higher melt temperature and cooling rate, producing smaller size grains hence raise the hardness of the manufactured part (Sateesh, Kumar, Prasad, C.K, & Vinod, 2014).

In addition, the sintered density reduces when the scanning speed increases (Kruth et al., 2010; A. Simchi & Pohl, 2003). Based on a microstructural analysis, when the scanning speed decreases, the energy density increases and the melt pool widens, thus increasing the overlapping of scan lines and leading to lower porosity percentages. Scanning speed also has a significant effect on the microstructure and dimensional accuracy of manufactured parts according to (Sateesh et al., 2014), who found that the dimensional accuracy decreases when the scanning speed increases. This happens because of the increasing melt temperature that leads to a decrease in molten metal viscosity and greater flowability. According to (Sateesh et al., 2014) also investigated the effects of density on the scanning speed parameter. They determined that the density decreases with increasing scanning speed. This can be explained

in terms of laser energy, where the laser energy density is proportional to the laser power and inversely proportional to the scanning speed.

The effects of scanning speed on yield strength and ultimate tensile strength were discussed by (Negi et al., 2015), who found that increasing the scanning speed decreases the yield strength and ultimate tensile strength. This phenomenon happened when the higher scanning speed applied, the energy absorbed by the melted material over a unit time and a unit area decreases, and thus improper sintering occurs due to insufficient energy delivered. Thus, the part strength deteriorates.

2.5.3 Hatching Distance

The hatching distance is the distance between two consecutive scan lines, as shown in Figure 2.4:

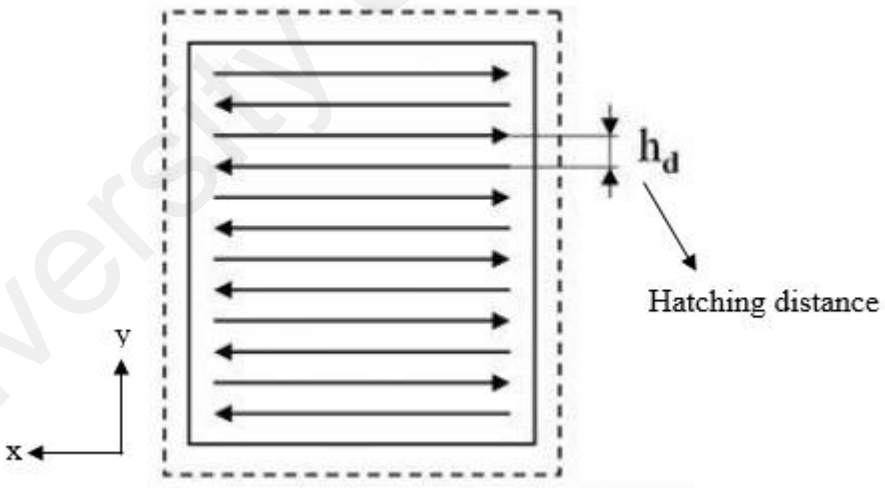

Figure 2.4: Illustration of hatching distance

Hatching distance is the main factor influencing the hardness and density of manufactured parts. Increasing the hatching distance leads to a detrimental effect that diminishes the hardness and density. Moreover, a greater hatching distance reduces the sintered density and overlapping of melt pools within the layer. Subsequently, the porosity percentage of the

manufactured part increases (A. Simchi & Pohl, 2003). However, increasing the hatching distance improves the production rate (Krishnan et al., 2014).

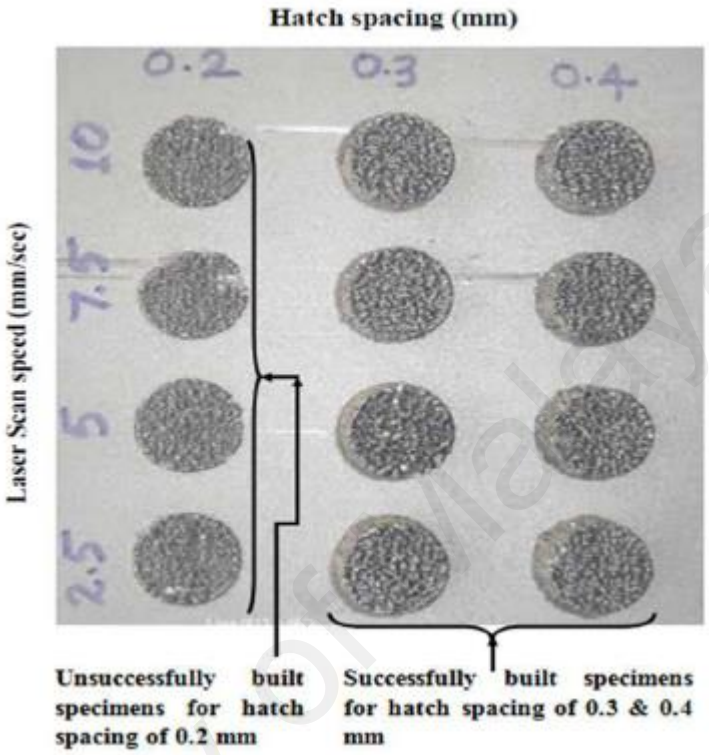

Figure 2.5: Laser-sintered Inconel 625

Hatching distance has significant effect on manufactured parts as seen in Figure 2.5, where a part with less than 0.3 mm was unsuccessfully built. The process cannot continue due to recoater blade jamming and balling that occurred on account of the lower hatching distance applied (Sateesh et al., 2014). In addition, lower hatching distance can lead to low hardness due to the larger grain size in the manufactured part (Sateesh et al., 2014). Furthermore, a smaller hatching distance causes an increase in energy density and possible curling on the manufactured part (Krishnan et al., 2014).

Hatching distance also impacts the strength of manufactured parts when (Negi et al., 2015) indicated that increasing the hatching distance reduces the strength of the parts manufactured. This can be justified by the fact that a high hatching distance leads to pack poorly of the

powder particles. For that reason, high chance of curling and clinging happened on the layer and causes the next layer from melting properly, which leads to poor part strength.

2.5.4 Building Direction

Building direction impacts the surface roughness more than the aforementioned process parameters. The mechanical properties, surface roughness and dimensional error of parts manufactured by direct metal laser sintering (DMLS) and SLM are subject to the process parameters applied, which are the scanning speed, layer thickness and building direction, as studied by (Delgado et al., 2011). Based on their discussion, building direction has significant impact on surface roughness obtained by DMLS and SLM. When the building direction was changed from low to high degree (0^o to 90^o), the surface roughness increased. According to the surface roughness measured in Figure 2.6, the top surface has less dimensional control so it is more accurate to measure the surface roughness on the X-Y plane than the lateral surface on the Y-Z plane.

Building direction additionally has strong influence on dimensional accuracy. When the building direction was changed from 0^o to 90^o, greater dimensional error was obtained in the width direction.

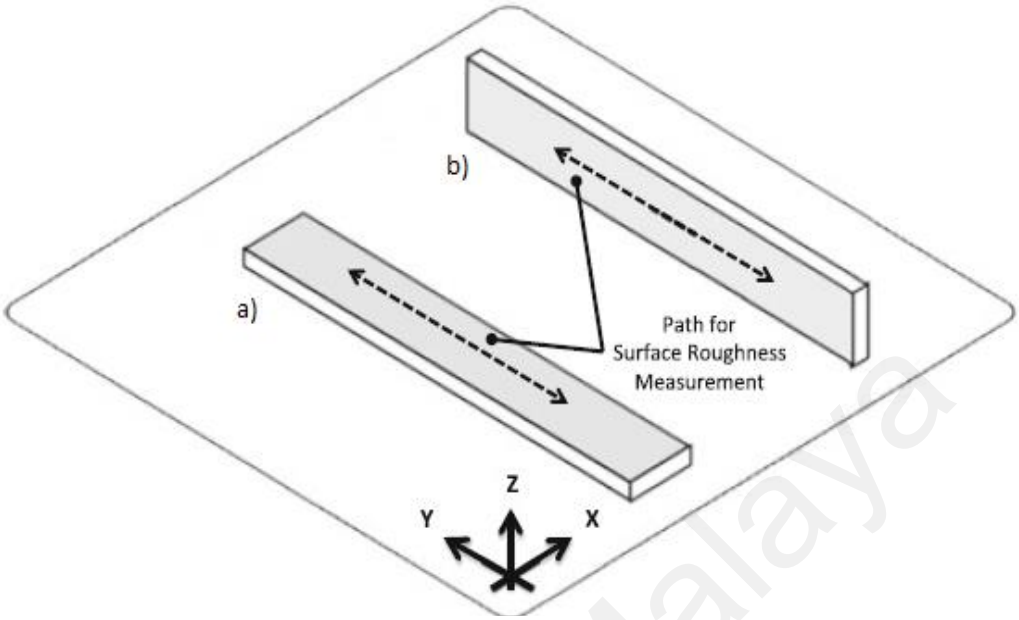

Figure 2.6: Surface roughness measurements at a) 0^o and b) 90^o

In recent years, the anisotropic tensile properties of parts manufactured by SLM have received much attention, particularly building direction (Guan, Wang, Gao, Li, & Zeng, 2013). The vertical building direction exhibits a great combination of ductility and strength, while the other side, horizontal building direction produces better tensile strength.

2.5.5 Layer Thickness

According to (Guan et al., 2013), the producibility of parts manufactured by SLM increases when thicker layers are applied, because the time to build the parts can be reduced while the tensile strength and ductility of the manufactured parts remain good. This is because layer thickness does not have a significant effect on the tensile strength and ductility of manufactured parts. Moreover, when the layer thickness increases, the balling phenomenon will occur due to insufficient energy density delivered to melt the powder. The presence of un-melted powder on the former melted layer may disturb the subsequent powder deposition process or it may cause the whole process to fail. Based on a microstructural study (Guan et

al., 2013) of the differences in layer thickness, no obvious difference was detected during observations of various layer thicknesses used. The slice thicknesses affect the surface

2.6 Design of Experiments

To investigate the interaction between parameters, a design of experiments (DOE) needs to be created. The relationship between various factors and the output can be determined by using DOE, since it is an organized and structured method (Phadke, 1995).

2.6.1 Taguchi Method

One of the DOE is the Taguchi method that is based on the experimental design arrangement otherwise known as orthogonal array design. The advantage of the Taguchi method is the minimal number of experiments required from a set of control factors. It is still an effective, efficient, simple and reliable means to attain optimum results. In this study, the response parameters affecting the mechanical properties can be optimized (Rahmati, Sarhan, & Sayuti, 2014).

There are a few stages in the Taguchi optimization, which include choosing the orthogonal array (OA) based on the number of controllable factors, starting the experiments by following the OA, analyzing the results, recognizing the optimum parameters using S/N ratios and ANOVA analysis, and conducting confirmation tests of the new optimum process parameters or factors. S/N ratios are known as log functions that serve as functions for optimization, assisting with data analysis and obtaining the preliminary or predicted output of the new optimum process parameters. S/N ratios are dependent on the experiment objectives (Jugulum & Samuel, 2008).

2.7 Shot Peening

Shot peening is a cold working process that is used as a finishing technique for metallic parts. The objective of this process is to prevent fatigue and corrosion, thereby increasing the life cycle of manufactured parts. It involves the use of small spherical shots, which are bombarded onto the surface of a part in other to obtain a better surface finish. The shot peening method has proven to be the most economical and effective way of producing surface residual compressive stresses, thus increasing the life span of treated metals. Furthermore, shot peening has been found to be a viable technique of enhancing the mechanical resistance of SLM parts, straightening distortions generated during production, and producing aerodynamic curvatures for aerospace applications (Frija, Hassine, Fathallah, Bouraoui, & Dogui, 2006; Torres & Voorwald, 2002) . In addition, other research works have indicated that the shot peening process could be used to enhance the surface quality of SLM manufactured parts (Calignano et al., 2012).

2.8 Summary of Literature Review

Based on the literature review, few investigations report on the parameter variations that influence the physic-mechanical properties of parts manufactured using SLM technology. Furthermore, little research has been conducted to improve the physic-mechanical properties of SLM manufactured parts. Hence, the focus in this research is on the parameters that may have greater influence on parts manufactured by SLM, namely laser power, scanning speed and hatching distance. In addition, the physic-mechanical properties are improved in this research to ensure that the quality of parts manufactured by SLM is comparable with that of solid materials produced using conventional methods.

CHAPTER 3 : METHODOLOGY

3.1 Introduction

This chapter describes the research methodology as shown in the flow chart in Figure 3.1. It also details the experimental process, including the design of experiment, experiment setup, equipment used, part fabrication and data collection.

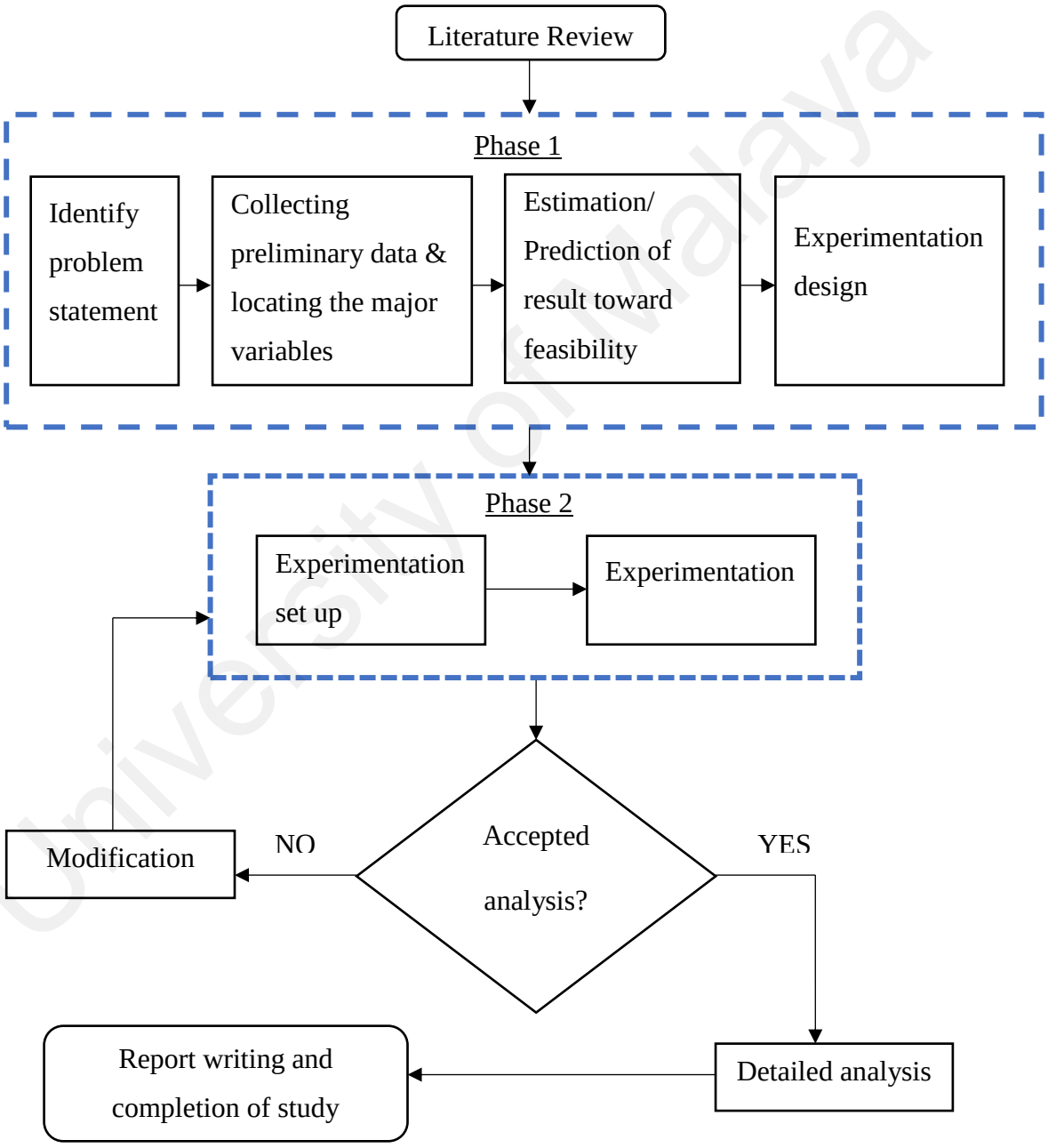

Figure 3.1: Flow chart of research methodology

3.2 Materials and Sample Preparation

In SLM, a laser source moves at a set scanning speed and selectively melts line-by-line each layer of powder material. The diameter of the physical beam is usually smaller than the diameter of the area where the particles are melted. The specifications and operation range of the SLM 280^{HL} machine used in this study are given in Table 3.1. The system software developed can perform functions such as transferring the CAD models in STL format to the layer data required by the machine. Besides, it can combine several parts to be manufactured on one building platform and select the drive data according to the different process requirements of each part.

Table 3.1: SLM 280^{HL} specifications

Building Platform (H x W x L)	365 mm^3 x 280 mm^3 x 280 mm^3
3D optics configuration/Dual configuration: with switching unit	Single (1x700 W), Twin (2x700 W), Dual (1x700 W and 1x1000 W); Single (1x400 W), Twin (2x400 W), Dual (1x400 W and 1x1000 W) IPG fiber laser
Powder materials available	Titanium, tool steel and stainless steel, aluminum, cobalt-chrome and nickel-based alloys
Weight (with/without powder)	approx. 1500 kg/ca. 1300 kg
Machine size (H x W x L)	2850 mm x 1050 mm x 3050 mm
Compressed air requirements/Consumption	ISO 8573-1:2010 [1:4:1], 50 l/min @ 6 bar
Power input/E-connection	400 Volt 3NPE, 32 A, 50/60 Hz, 3.5 – 5.5 kW
Gas consumption purging (average)	70 l /min (argon)
Gas consumption in process (average)	2.5 l/min (argon)
Minimum feature size	150 µm
Building rate	Up to 55 cm^3/h
Laser beam diameter	80 - 115 µm
Layer thickness	20 µm - 75 µm
Maximum scanning speed	10 m/s

The material used in this study is stainless steel 316 L (SS316L). Initial observations were made by Field Emission Scanning Electron Microscopy (FESEM) with Energy Dispersion X-ray Spectroscopy (EDS) to determine the morphology and chemical composition of the SS316L powder particles. The particles' size and shape highly affect the sinter-ability and flowability, which are related to the powder layer deposition.

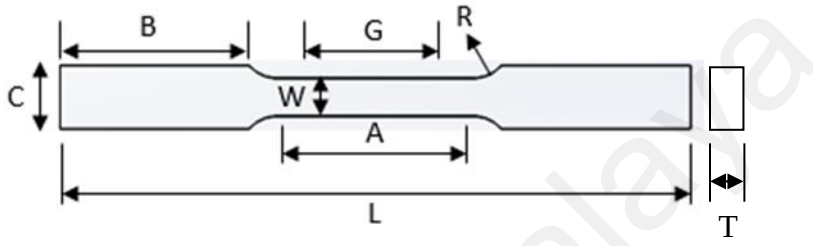

Figure 3.2: Drawing of part used for testing

Table 3.2: Dimensions of manufactured part

Characteristics of part	**Length (mm)**
Gage length, G	25
Width, W	6
Width of grip section, C	2
Fillet radius, R	6
Overall length, L	100
Length of reduced section, A	32
Length of grip section, B	30
Thickness, T	2

Figure 3.2 illustrates the test part designed for this research work. It was designed according to ASTM E8/E8M standards for rectangular tension testing of metallic materials as described in Table 3.2.

3.3 Design of Experiments

The design of experiments (DOE) was set up to determine the relationship between factors affecting a process and the process output. This information is needed to manage the process inputs in order to optimize the output.

Table 3.3: Process parameters

Parameter	Units	Symbol	Level			
			1	2	3	4
Laser Power	**Watts (W)**	**P**	120	200	275	360
Scanning Speed	**mm/s**	**v**	250	510	760	900
Hatching distance	**mm**	**h_d**	0.08	0.10	0.12	0.14

The laser power, scanning speed and hatching distance employed are stated in Table 3.3. These three parameters were chosen based on standard machine laser power, scanning speed and hatching distance reported by the machine manufacturers. Moreover, both layer thickness and laser focus diameter were kept constant as 50 µm and 80 µm, respectively. The variations in process parameter values depend on the limitations of the machine used in the experiments. Other parameters that have potential effects on surface roughness were kept constant, as these parameters are outside the scope of the study.

Before conducting the experiment, the design of experiment was set up. For this study, the Taguchi method was used to conduct the experiment, which is based on the orthogonal array design. This design provides reduced variance in the experimentation process with optimum control parameter settings. The S/N ratios are the log functions utilized to find the optimum parameter settings. They also help with data analysis and predicting the optimum results.

According to the full factorial technique, 64 tests should be done and that would be time-consuming and costly. Hence, the Taguchi method reduces the number of experiments from 64 to 16. The Taguchi experimental design with three control factors and four levels each (Table 3.4) was prepared to determine the effectiveness of the selected parameters on the manufactured part properties. This was done using the design of experiments and analysis in MINITAB software. The experiment was designed based on the L_{16} orthogonal array with the Taguchi method. To assure the accuracy of the results obtained from the experiments, each experiment was repeated three or five times, and the average of the results was taken. Furthermore, ANOVA statistical analysis and S/N ratios were applied to evaluate the factors that influence the properties of the manufactured part.

Table 3.4: Taguchi design

No	**P (W)**	**v (mm/s)**	**h_d (mm)**	**E_d (J/mm^2)**
1	120	250	0.08	6.00
2	120	510	0.10	2.35
3	120	760	0.12	1.32
4	120	900	0.14	0.95
5	200	250	0.10	8.00
6	200	510	0.08	4.90
7	200	760	0.14	1.88
8	200	900	0.12	1.85
9	275	250	0.12	9.17
10	275	510	0.14	3.85
11	275	760	0.08	4.52
12	275	900	0.10	3.06
13	360	250	0.14	10.29
14	360	510	0.12	5.88
15	360	760	0.10	4.74
16	360	900	0.08	5.00

3.4 Testing

3.4.1 Surface roughness

The surface roughness of each sample was obtained accordingly to the ANSI Mitutoyo Surftest SJ-210 surface roughness tester standard (Figure 3.3). The surface roughness value (R_a) was measured three times at three different locations (on top). To ensure result accuracy, every experiment was repeated three times and the average of the results was taken.

Figure 3.3: Mitutoyo Surftest SJ-210

3.4.2 Dimensional accuracy

Dimensional accuracy in additive manufacturing describes the geometrical difference between a virtually designed CAD part and a physical part after the building process Dimensional errors occurred when the dimensional accuracy does not meet the quality target, or the accuracy worsens. Dimensional accuracy is one of the main concerns in AM technologies (Lee, Chung, Lee, Yoo, & Ko, 2014), whereby it is important for the manufactured parts to be designed for products that can fit tightly with each other, especially in the biomedical industry. SLM process can be checked by comparing the features of the parts, such as cylinders, rectangular slots and angles (Kamarudin, Wahab, Raus, Ahmed, & Shamsudin, 2017).

Dimensional measurements were made with an Oxford precision micrometer with 0.01 resolution and 0-25 mm measurement range. The thickness of the manufactured part was measured as in Figure 3.4 and the dimensional accuracy was calculated with Equation (3.1):

$$\text{Dimensional accuracy (\%)} = \left| \frac{\text{thickness}_{\text{theoretical}} - \text{thickness}_{\text{experimental}}}{\text{thickness}_{\text{theoretical}}} \right| \text{x } 100\ \% \qquad (3.1)$$

Figure 3.4: Oxford precision micrometer

3.4.3 Tensile testing

In the basic tensile test, a specimen is subjected to controlled tension until failure. This type of test is used to select for quality control, for an application, and to predict the behaviour of a material when certain forces are applied. Normally, the ultimate tensile strength (UTS), reduction in area (RA) and maximum elongation (EL) can be measured through tensile testing. According to the results, other properties can be measured as well, such as Young's modulus (E), yield strength (σy), Poisson's ratio (v), and strain hardening characteristics ASTM E8/E8M was used to determine the tensile strength of the metallic materials at room temperature. The tensile strength was tested by INSTRON universal testing machine at 0.05 mm/min testing speed and 30 kN maximum force, as shown in Figure 3.5:

Figure 3.5: INSTRON universal testing machine

3.4.4 Hardness

Hardness test is to determine the hardness of the solid matter when some of a compressive force is applied where, metal materials are stronger/harder than other materials. Generally, macroscopic hardness is characterized by strong **i**ntermolecular bonds, but the reaction of solid materials under force is complex. Hence, few others measurements are doneto obtain the material hardness such as scratch hardness, rebound hardness and indentation hardness. The hardness performance is dependent on elastic stiffness, ductility, plasticity, strength, strain, viscosity, viscoelasticity and toughness.

Hardness testing is one of the steps required to check the quality of parts manufactured using SLM. A Vickers Hoytom Minor-69 hardness tester was used to analyze the hardness of the manufactured part, as illustrated in Figure 3.6. To obtain the average hardness of the manufactured part, five measurements were taken in different areas. The testing was done accordingly to ISO 6507-1:2005 standard.

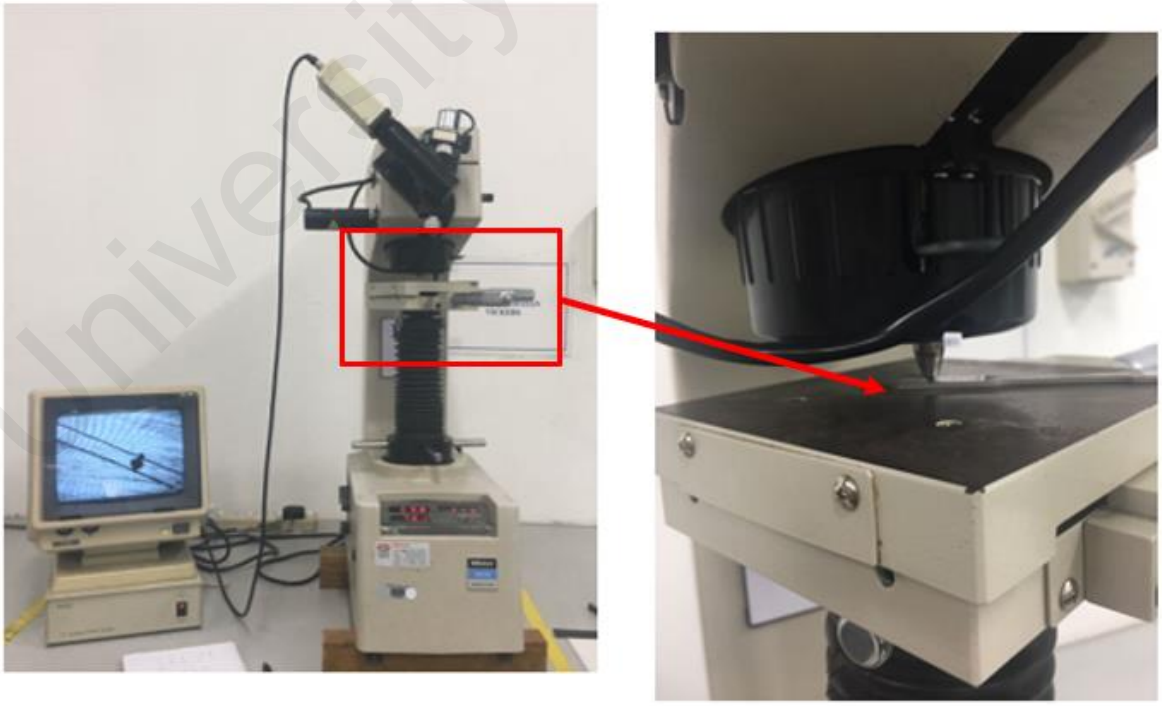

Figure 3.6: Vickers Hoytom Minor-69

3.4.5 Porosity

The density and porosity of the manufactured part were measured by volumetric method. The mass of each manufactured part was measured in air and water three times with an electronic balance and the average mass was calculated. An initial water volume of 20 mL was added to a cylinder and then the manufactured part was immersed in the water. The final volume was measured. The density of the manufactured part was calculated with Equation (3.2):

$$\rho_{experiment} = \frac{m_a}{V_f - V_i} \tag{3.2}$$

Where $\rho_{experiment}$ is the manufactured part density, V_f is the final volume and V_i is the initial volume. The difference between the theoretical and experimental density is termed porosity. Equation (3.3) was used to calculate the percentage of porosity in the manufactured part.

$$\text{Porosity (\%)} = \left| 1 - \frac{\rho_{experiment}}{\rho_{theoretical}} \right| \text{ x } 100\% \tag{3.3}$$

where $\rho_{experiment}$ is the density of the manufactured part and $\rho_{theoretical}$ is the density of stainless steel 316L, which is 8 g/cm^3.

3.5 Shot Peening

In order to improve the mechanical properties of the manufactured part, shot peening was applied for 6 parameter settings (i.e. six experiments) using a Peenmatic 620 S machine (Figure 3.7) at 4 bars of pressure. Next, the R_a before and after shot peening was analyzed to find the variation.

Figure 3.7: Peenmatic 620 S machine

3.7 Data Analysis

ANOVA statistical analysis and S/N ratio were applied to evaluate the factors that influence the properties of the manufactured part. The S/N ratio is a log function used to find the optimum parameter settings. It also helps with the data analysis and in predicting the optimum results. The design of experiment and analysis were done using MINITAB software.

CHAPTER 4 : RESULTS AND DISCUSSION

4.1 Powder Analysis

The SS316L metal powder underwent gas atomization due to the suitability of this process for producing materials for additive manufacturing technologies (Kearns & Murray, 2010). The morphology and chemical composition of the SS316L powder particles were obtained using field emission scanning electron microscopy (FESEM) with energy dispersion x-ray spectroscopy (EDX). Moreover, the shape and size of the powder particles were observed due to the high effect they have on the sinter-ability and flow-ability of the material. According to Figure 4.1, the shape of the particles seems to be spherical and it is agglomerates to each other between tiny powder particles with bigger powder particles. The average of the particle size distribution of the powders is 30 µm. The chemical composition of the powder particles observed with the aid of EDX is given in Table 4.1.

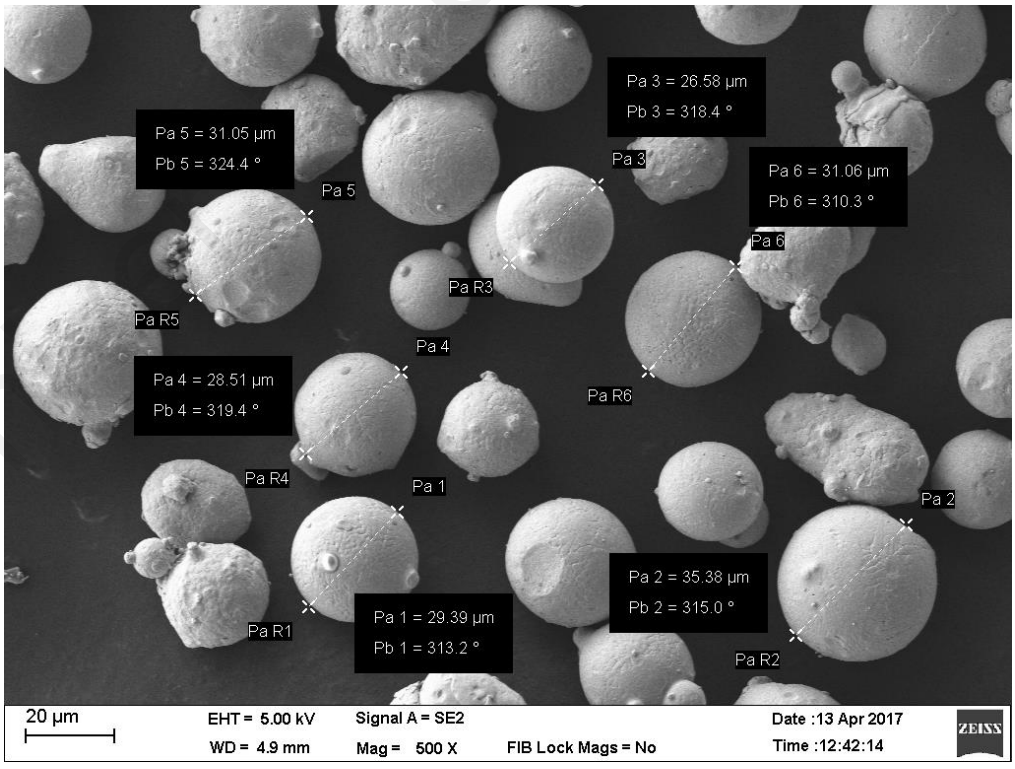

Figure 4.1: FESEM micrographs of SS316L metal powder before melting at 500x magnification

Table 4.1: Chemical composition of SS316L

Element	**Carbon, C**	**Iron, Fe**	**Nickel, Ni**	**Silicon, Si**	**Molybdenum, Mo**	**Chromium, Cr**
Wt %	00.66	55.56	15.65	00.82	04.29	22.00
At %	02.90	52.75	14.14	01.54	02.37	22.44

4.2 Data Analysis

The parts were produced under different process parameter settings according to the Taguchi L_{16} array. The optimum parameters were determined by calculating the S/N ratio. The S/N depends on whether the mean-squared deviation is a number less or greater than 1, i.e. whether S/N is positive or negative (Calignano et al., 2012). Moreover, to find the most significant parameters that affect the properties of manufactured parts, Analysis of Variance (ANOVA) was conducted. ANOVA indicated the parameters with the highest influence on the part properties by comparing their p-values, which were below the 0.05 significance level.

4.2.1 Surface Roughness

In terms of R_a, the-lower-the-better problem was utilized in the analysis to obtain a better surface finish. The R_a values from the experiment was tabulated in Table 4.2 with the S/N ratio values were calculated by using the logarithmic relationship given in Equation (4.1) and are listed in Table 4.2.

$$S/N=-10x\log\left(\sum (Y_i^2)/n\right) \quad (4.1)$$

Where Y is the experimentally observed value in the i^{th} experiment and n is the number of times each experiment was repeated.

Table 4.2: Experiment, R_a and S/N ratio results based on different process parameter combinations using the L_{16} array

No	P, W	v, mm/s	h_d, mm	R_a 1, µm	R_a 2, µm	R_a 3, µm	Average R_a, µm	S/N ratio
1	120	250	0.08	9.64	9.87	10.24	9.92	-19.93
2	120	510	0.1	10.69	12.16	11.75	11.53	-21.24
3	120	760	0.12	9.48	10.16	10.75	10.13	-20.11
4	120	900	0.14	10.12	10.48	9.73	10.11	-20.10
5	200	250	0.1	13.21	14.16	11.53	12.97	-22.26
6	200	510	0.08	11.65	12.32	13.52	12.50	-21.94
7	200	760	0.14	13.14	10.90	11.14	11.72	-21.38
8	200	900	0.12	11.20	11.60	10.83	11.21	-20.99
9	275	250	0.12	18.47	18.24	18.93	18.55	-25.37
10	275	510	0.14	20.26	21.51	18.47	20.08	-26.06
11	275	760	0.08	16.92	13.35	13.01	14.43	-23.18
12	275	900	0.1	11.12	12.28	10.49	11.30	-21.06
13	360	250	0.14	33.57	32.91	40.78	35.75	-31.07
14	360	510	0.12	23.40	27.86	20.91	24.06	-27.62
15	360	760	0.1	30.65	26.21	27.75	28.20	-29.01
16	360	900	0.08	25.75	14.58	20.08	20.13	-26.08

A sufficient amount of energy (energy density) is needed to deliver the powder on the part's bed surface in order to produce a good, functional melted part. If the amount of energy is insufficient, a poor bond neck may form between the powder particles. Thus, the surface finish can be enhanced by increasing the energy density up to an optimum level (Cherry et al., 2015).

The ANOVA analysis for S/N ratio is presented in Table 4.3. To determine which parameters were the most significant on the surface quality of the manufactured part, the p-values of the parameters were compared. According to the table, it appears that the laser power factor has the highest influence on surface quality because it has the lowest p-value (<0.05 significance level).

Table 4.3: ANOVA analysis for S/N ratios (surface roughness, R^2 = 95.64%)

Source	DF	Adj SS	Adj MS	F-Value	P-Value
Laser power	3	151.99	50.67	38.11	0.00
Scanning speed	3	15.61	5.20	3.91	0.07
Hatching distance	3	7.28	2.43	1.83	0.24
Error	6	7.98	1.33	-	-
Total	15	182.86	-	-	-

The average of each characteristic (S/N ratio) at every factor level was calculated by the ANOVA and it is tabulated in Table 4.4. The factor ranking is based on the delta statistic that compares the relative magnitude of the effects. The delta value was obtained by subtracting the highest average value of each factor from the lowest average value. Rank 1 has the highest delta value, followed by rank 2 and rank 3. Based on the S/N ratio results, it can be concluded that laser power has the greatest influence on the surface quality of the manufactured part, followed by scanning speed and then hatching distance.

Table 4.4: Response table for surface roughness

Level	Laser Power, W	Scanning speed, mm/s	Hatching distance, mm
1	-20.34	-24.65	-22.78
2	-21.64	-24.21	-23.39
3	-23.92	-23.42	-23.52
4	-28.44	-22.06	-24.65
Delta	8.10	2.60	1.87
Rank	1	2	3

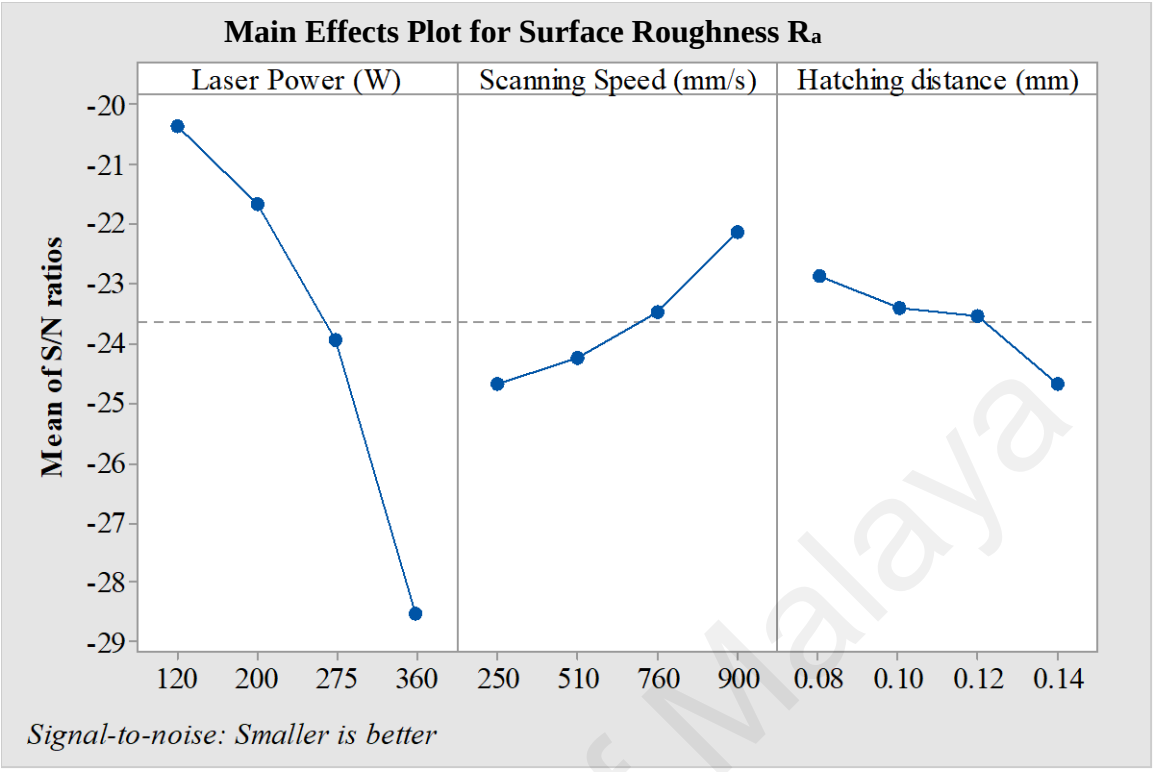

Figure 4.3: Main effect plot surface roughness

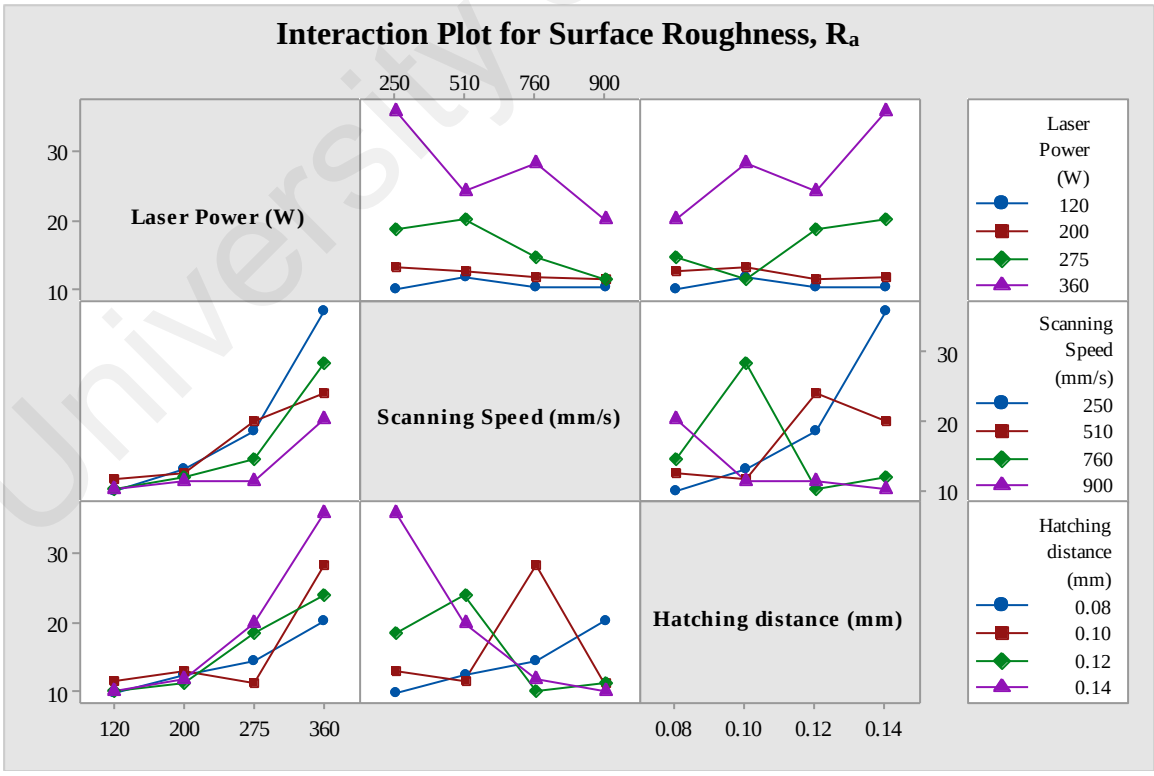

Figure 4.2: Interaction plot for surface roughness

Figure 4.2 contains the main effect plot for S/N ratio that was used to verify the statistical results obtained. The table displays the response mean for each factor level. In addition, a horizontal line is drawn at the grand mean and the slopes of the lines relating to the process parameter levels indicate the effect of each process parameter. It can be seen that the optimum surface roughness was achieved when the laser power was 120 W, the scanning speed was 900 mm/s and the hatching distance was 0.08 mm.

The interaction between each of the input variables and the surface quality of the manufactured part is shown in Figure 4.3. Lines that are parallel in the interactions plot indicate there is no interaction between the given parameters. However, the higher the degree of line intersection and the less parallel the lines are with one another, the higher the degree of interaction is. Based on the graph, when the laser power and hatching distance values are low and the scanning speed value is high, the possibility of obtaining a low R_a value is high. Scanning speed and hatching distance evidently have a good interaction towards achieving a good surface finish. Moreover, it is clear there is a strong relationship and interaction between laser power and scanning speed when the laser power is less than 200 W.

Equation (2.1) indicates there is a directly proportional relationship between energy density and laser power, and an inversely proportional variation relationship between hatching distance and scanning speed with energy density. As such, whenever the laser power is increased and the other two factors are decreased, there seems to be an imminent increase in the powder temperature. Since there is a temperature gradient between the solidifying zone and the laser beam when the laser moves, the increase in temperature creates a shear force on the liquid surface that is contrasted by the surface tension of the melted liquid (Ho, Cheung, & Gibson, 2002). The interlayer connection and wettability of the melt can then be improved by applying higher laser power, due to its ability to flatten the melted pool. The

tendency of the balling effect to occur can be reduced by improving the wettability due to the diminished variations in surface tension. However, if laser power is set too high, large amounts of material may vaporize and recoil pressure may occur that will cause disruptions to the melt pool surface and thereby increasing the R_a (Stwora & Skrabalak, 2013). When an optimum scanning speed is utilized, the top surface finish can be improved. This is because the melt pool will have more time to flatten before solidification with the help of gravity and surface curvature forces that counteract the external shear forces. Moreover, larger volumes of liquid produced within the melt pool are also achievable by utilizing low scanning speed. The reason is that the increased liquid volume has a tendency to widen the melt pool, thereby causing larger thermal differences across it and consequently varying the surface tensions. In addition, using optimum scanning speed causes the non-melted particle cores to bake together into coarsened balls with a diameter almost the same as that of the beam. To minimize these changes, the melt pool may break off into smaller entities -- which is known as "balling," thereby solidifying the edge of the melt pool and thus increasing the surface roughness, R_a. Optimal parameters allow stabilizing thermal processes, consequently avoiding the balling effect.

4.2.2 Dimensional Accuracy

The dimensional accuracy values of the parts are listed in Table 4.5. After evaluating the response, ANOVA analysis was conducted to determine the highest influence on the accuracy of the manufactured parts. The optimum parameters were determined using the lower-the-better approach of dimensional error percentage as in Equation (4.1). The dimensional accuracy was calculated with Equation (4.2).

$$\text{Dimensional Accuracy \%} = \left|\frac{A_0 - A_1}{A_0}\right| \quad (4.2)$$

Where A_0 is the design size given by the computer and A_1 is the actual size measured by a micrometer screw gauge.

Based on the table below, the average thickness of the manufactured parts for each setting parameter is higher than the drawing value (2 mm). The results also clearly show that higher dimensional error occurred when the energy density was increased. The energy density is related to the process parameters applied, namely laser power, scanning speed and hatching distance.

Table 4.5: Dimensional accuracy and S/N ratio results

No	P, W	v, mm/s	h_d, mm	D1, mm	D2, mm	D3, mm	Average, mm	Dimensional Accuracy, %	S/N Ratio
1	120	250	0.08	2.09	2.08	2.13	2.11	5.67	-15.07
2	120	510	0.1	2.10	2.10	2.11	2.10	5.17	-14.26
3	120	760	0.12	2.08	2.10	2.13	2.10	5.17	-14.26
4	120	900	0.14	2.07	2.10	2.10	2.09	4.56	-13.17
5	200	250	0.1	2.13	2.19	2.10	2.14	7.00	-16.90
6	200	510	0.08	2.08	2.10	2.09	2.12	6.00	-15.56
7	200	760	0.14	2.11	2.13	2.10	2.11	5.67	-15.07
8	200	900	0.12	2.10	2.10	2.09	2.10	4.89	-13.78
9	275	250	0.12	2.10	2.20	2.28	2.19	9.61	-19.66
10	275	510	0.14	2.14	2.15	2.13	2.28	14.15	-23.02
11	275	760	0.08	2.26	2.27	2.28	2.27	13.44	-22.58
12	275	900	0.1	2.15	2.11	2.11	2.12	6.11	-15.72
13	360	250	0.14	2.67	2.68	2.43	2.59	29.67	-29.45
14	360	510	0.12	2.21	2.26	2.21	2.55	27.67	-28.84
15	360	760	0.1	2.42	2.41	2.39	2.50	25.17	-28.02
16	360	900	0.08	2.36	2.27	2.28	2.30	15.17	-23.62

The ANOVA analysis of S/N ratios is presented in Table 4.6. To determine which parameters were the most significant on the surface geometry of manufactured parts, the p-values of the parameters were compared. The table indicates that laser power is the factor with the greatest influence on manufactured part accuracy because it has the lowest p-value (<0.05 significance level).

Table 4.6: ANOVA analysis of S/N ratios (dimensional accuracy, R^2 = 96.65%)

Source	DF	Adj SS	Adj MS	F-Value	P-Value
Laser Power	3	438.63	146.21	52.39	0.00
Scanning Speed	3	40.34	13.45	4.82	0.05
Hatching Distance	3	4.52	1.51	0.54	0.67
Error	6	16.75	2.79	-	-
Total	15	500.23	-	-	-

The average of each characteristic (S/N ratio) at every factor level is given in Table 4.7. Based on the results, it can be concluded that laser power has the most influence on manufactured part accuracy, followed by scanning speed and hatching distance.

Table 4.7: Response table for dimensional accuracy

Level	Laser Power, W	Scanning speed, mm/s	Hatching Distance, mm
1	-14.19	-20.27	-19.20
2	-15.33	-20.42	-18.73
3	-20.24	-19.98	-19.14
4	-27.48	-16.57	-20.17
Delta	13.29	3.85	1.45
Rank	1	2	3

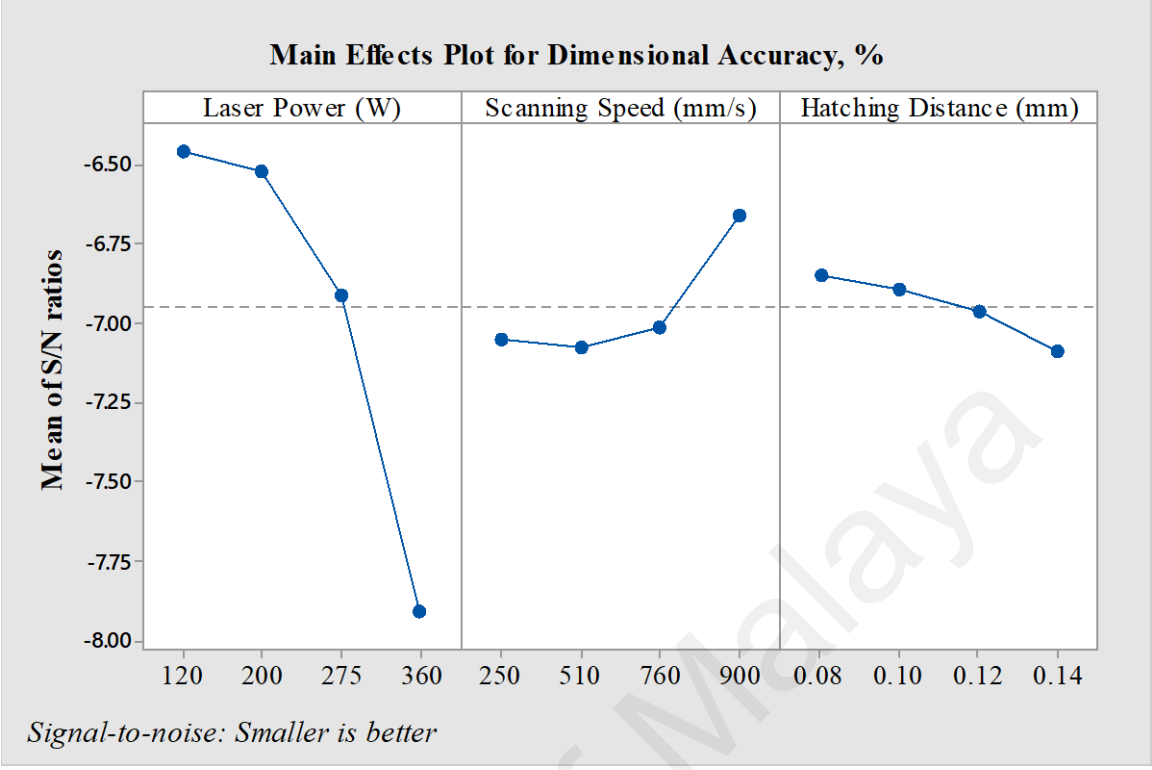

Figure 4.4: Main effects plot for dimensional accuracy, %

Figure 4.4 shows the main effects plot for S/N ratios that was used to verify the statistical results obtained. Based on the figure, there is a huge gap in dimensional accuracy between 275 W and 360 W laser power applied. This happened due to the increase in melt temperature, which led to a decrease in the viscosity of molten metal and an increase in flowability. Moreover, it is evident that the optimum dimensional accuracy was obtained when the laser power was 120 W, the scanning speed was 900 mm/s and the hatching distance was 0.08 mm.

The main cause of part inaccuracy was the swelling during melting, which does not always take place uniformly. In addition, the high process temperature coupled with the melt pool size and surface tension has a tendency to swell more than lower temperature, while part geometries like thick walls or sections can boost the swelling phenomenon (Bin & B, 2015). Besides, more solidified metal over the metal powder will lead to swelling on the

manufactured part. Another reason swelling happens is that when the next layer to the powder touches the building platform or previous layer, it quickly solidifies according to the thermal properties and temperature of the substrate. Due to the different thermal boundary conditions, the evolution of roads in the first layer differs from that in successive layers.

4.2.3 Tensile Strength

A tensile test was conducted on the manufactured parts and the results are tabulated in Table 4.8. After evaluation, ANOVA analysis was used to determine the process parameters with the highest influence on the strength of the manufactured parts. The optimum parameters for manufactured part strength were determined using the larger-the-better approach for S/N ratios according to Equation (4.3):

$$S/N=-10x\log\left(\sum\left(\frac{1}{Y_i^2}\right)/n\right) \quad (4.3)$$

Where Y is the experimentally observed value in the i^{th} experiment and n is the number of times each experiment was repeated. The results were compared with stainless steel 316L from ASTM A240/A240M, which the ultimate tensile strength is 485 MPa.

Table 4.8:Tensile strength and S/N ratio results

NO	P, W	v, mm/s	h_d, mm	UTS 1, MPa	UTS 2, MPa	UTS 3, MPa	Average MPa	S/N Ratio
1	120	250	0.08	502.13	341.08	500.38	447.86	53.02
2	120	510	0.1	342.05	349.08	355.69	348.94	50.86
3	120	760	0.12	249.94	249.15	234.84	244.65	47.77
4	120	900	0.14	188.92	191.63	197.90	192.82	45.70
5	200	250	0.1	507.70	518.52	496.13	507.45	54.11
6	200	510	0.08	566.743	526.33	514.81	535.96	54.48
7	200	760	0.14	236.88	233.90	255.98	242.26	47.69
8	200	900	0.12	268.87	265.97	286.04	273.62	48.74
9	275	250	0.12	500.22	499.93	514.87	505.01	54.07
10	275	510	0.14	365.52	434.82	416.97	405.77	52.17
11	275	760	0.08	489.57	486.81	487.28	487.89	53.77
12	275	900	0.1	525.73	510.52	465.56	500.60	53.99

Table 4.8, continued

13	360	250	0.14	470.69	469.61	472.61	470.97	53.46
14	360	510	0.12	505.43	507.74	505.28	506.15	54.09
15	360	760	0.1	482.60	384.48	425.90	431.00	52.69
16	360	900	0.08	141.51	391.48	442.18	325.06	50.24

Based on the comparison, some manufactured parts exhibited better tensile strength. This is a general feature of many laser-processed materials due to the high cooling rate, which always leads to a fine microstructure with high dislocation density (B. Song, Dong, Deng, Liao, & Coddet, 2014). For example,(Guan et al., 2013) showed that the tensile strength of 304 stainless steel parts manufactured by SLM was 714-717 MPa, which is higher than ASTM A240/A240M 304 steel with 515 MPa. Moreover, (Kempen, Thijs, Van Humbeeck, & Kruth, 2012) found that the tensile strength of AlSi10Mg parts produced by SLM (396 MPa) is comparable to, or even exceeds that of conventionally cast AlSi10Mg samples (300 MPa). But, some of manufactured parts yield poor tensile strength compared to wrought products. The reason is the low density and huge number of cavities within, which may weaken the strength of manufacture parts.

Table 4.9: ANOVA analysis for S/N ratios (tensile strength, R^2 = 92.67%)

Source	DF	Adj SS	Adj MS	F-Value	P-Value
P (W)	3	39.40	13.13	8.99	0.01
v (mm/s)	3	43.63	14.54	9.96	0.01
h_d (mm)	3	27.69	9.23	6.32	0.03
Error	6	8.77	1.46	-	-
Total	15	121.19	-	-	-

The ANOVA analysis for S/N ratios according to the larger-the-better principle is provided in Table 4.9. The p-values were compared to determine which parameter has the biggest impact on manufactured part strength. Based on the data analysis in Table 4.9, three factors

have the greatest influence on the strength of manufactured parts on account of the lowest p-value (below 0.05 significance level).

Next, the average of each characteristic (S/N ratio) at every factor level is shown in Table 4.10. Based on the S/N results, it can be concluded that laser power and scanning speed are the highest influence on the strength of manufactured parts, followed by hatching distance.

Table 4.10: Response table for tensile strength

Level	Laser Power (W)	Scanning speed (mm/s)	Hatching Distance (mm)
1	49.34	53.66	52.90
2	51.28	52.92	52.91
3	53.50	50.48	51.17
4	52.62	49.67	49.75
Delta	4.16	4.00	3.16
Rank	1	2	3

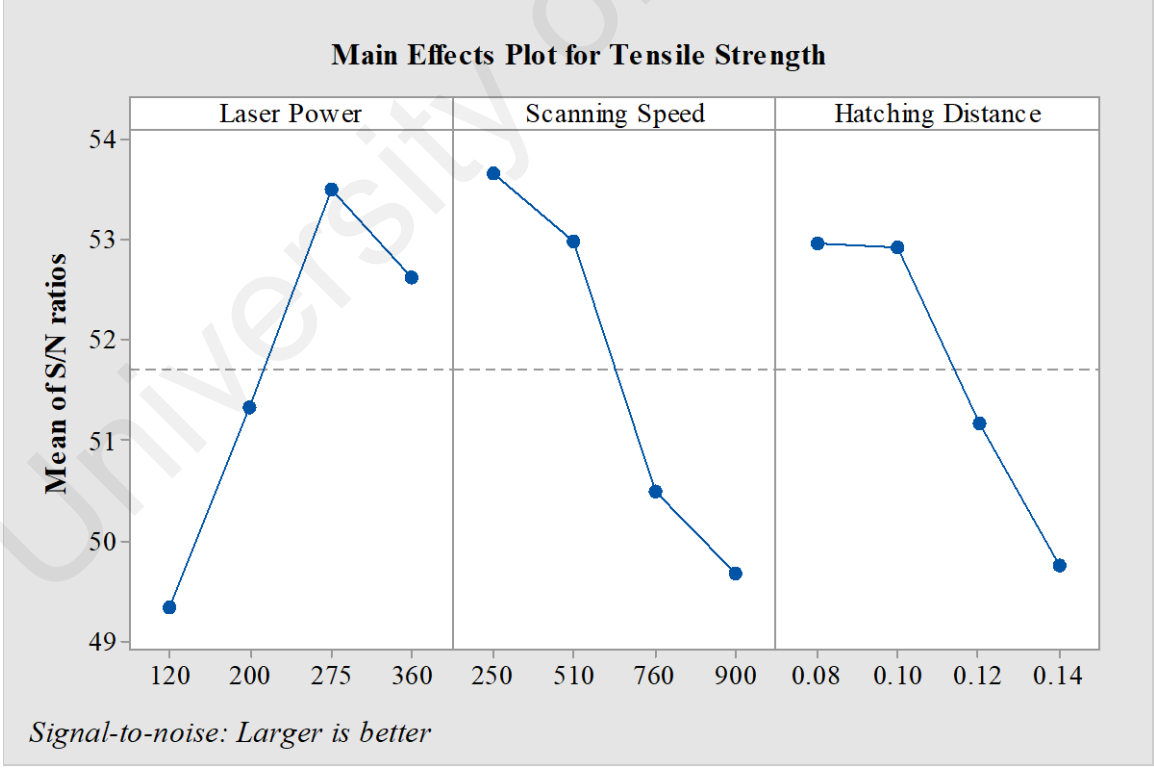

Figure 4.5: Main effects plot for tensile strength

Figure 4.5 displays the main effects plot for S/N ratios that was used to verify the statistical results obtained. It is clear that the optimum parameters for tensile strength were obtained when the laser power was 275 W, the scanning speed was 250 mm/s and the hatching distance was 0.08 mm.

Increasing the laser power from low to high levels increased the ultimate tensile strength of part manufactured. It happened due to high laser power when the energy transferred to the powder material to ensure it melted properly, thus generating a closely packed model and leading to enhanced part strength. Furthermore, greater laser power raises the melt temperature, while higher melt temperature speeds up the cooling rate and leads to reduced grain size. However, if the laser power is kept high, the tensile strength decreases owing to the enlarged grain size, which is known as a severe undercut and humping effect (Makoana, Möller, Burger, Tlotleng, & Yadroitsev, 2016).

In this study it was found that with a faster scanning speed tends to weaken the strength of the manufactured parts. This phenomenon happened when the high scanning speed applied, the energy absorbed by the sintered material over a unit time and a unit area decreases, and thus leads to improper melting due to insufficient energy delivered. Hence, it reduced part strength.

It was also found in this study that increasing the hatching distance reduced the strength of the parts manufactured as discussed in (Negi et al., 2015). This can be justified by the fact that a high hatching distance leads to pack poorly of the powder particles. For that reason, high chance of curling and clinging on the layer happened and causes the next layer from melting properly, which leads to poor part strength.

As far as the mechanical behaviour of SLM parts is concerned, it was shown that they have higher tensile strength and at the same time comparable ductility and lower fatigue life than parts produced via traditional manufacturing processes. Hence, from this perspective, the SLM process that allows the retention of self-strengthening mechanisms is opening great potential for the fabrication of industrial parts.

4.2.4 Fracture Toughness

Defects, such as pickup of impurities like nitrogen and oxygen, pores and brittleness of the manufactured part deteriorate the toughness of parts manufactured by SLM.

a)

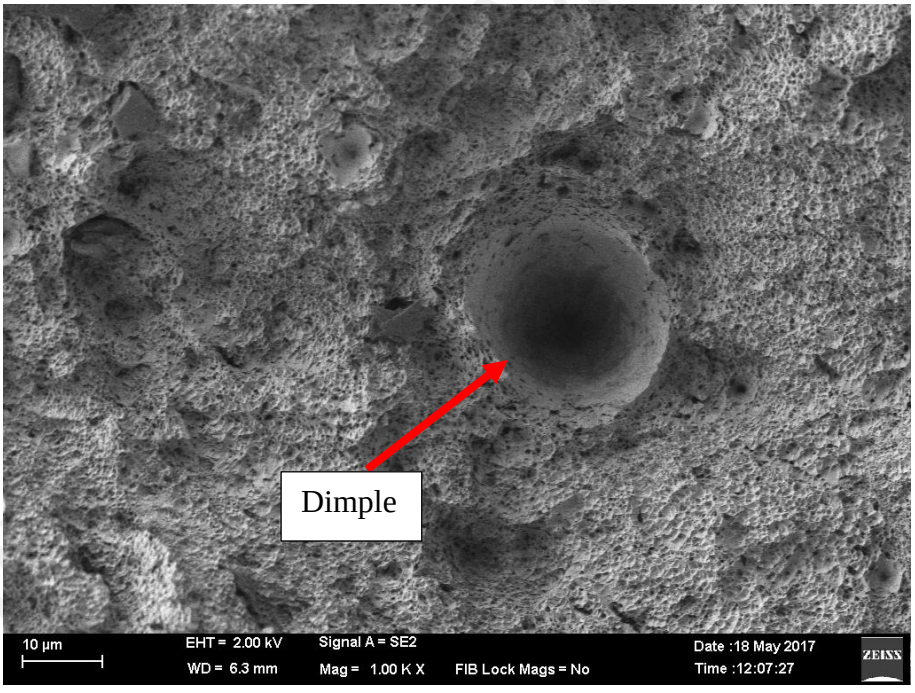

b)

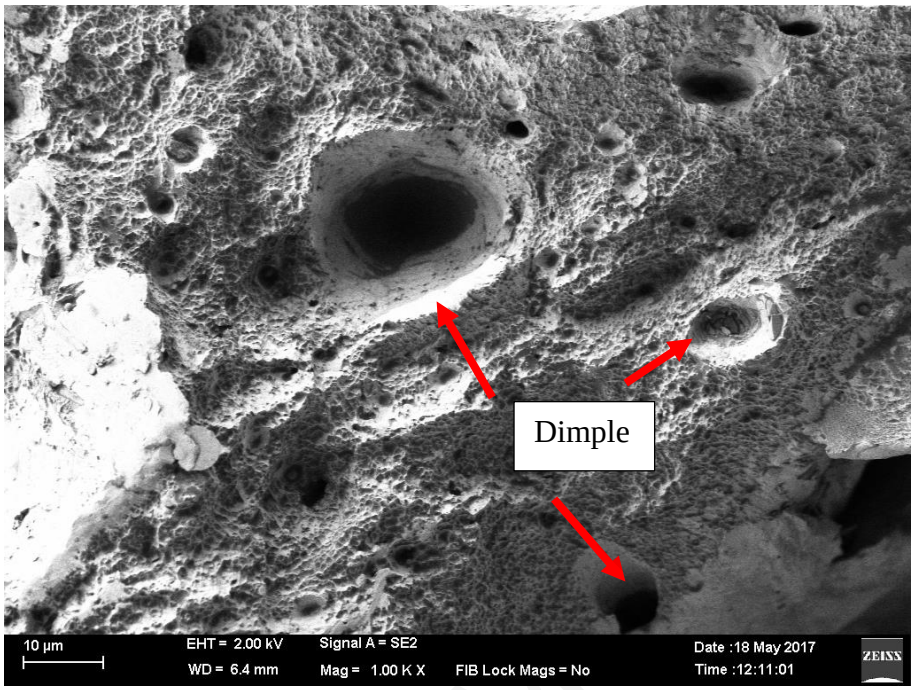

Figure 4.6: Fracture morphologies at laser power of 200 W with different laser scanning speeds and hatching distances: a) 510 mm/s scanning speed and 0.08 mm hatching distance, and b) 760 mm/s scanning speed and 0.14 mm hatching distance

Figure 4.6 represents typical tensile fracture surfaces of SLM-processed iron specimens using two scanning speeds (510 and 760 mm/s) and hatching distances (0.08 and 0.14 mm) and laser power of 200 W. The central area of the fractured part is commonly described as a region of fibrous fractures (Krakhmalev et al., 2016). FESEM analysis revealed that the fractured surface in the fibrous zone of the manufactured part is quite irregular and not horizontal due to the presence of initial porosity in the SLM specimens. A highly irregular fracture surface implies intensive crack deflection during tension. For example, when the pores and the micro voids coalesced, they formed not only horizontal but also inclined surfaces. Another reason for the irregular fractured surface could be residual stresses affecting crack propagation locally. Moreover, the FESEM analysis indicated the formation of dimples and dimpled rupture fractures in the fibrous zone in Figures 4.6 (a) and (b). The ductile fracture mechanisms in the necking region are usually associated with pore coalescence.

Figure 4.6(b) illustrates several dimple-like features corresponding to the high plastic deformation that occurred before the rupture. Rupturing was due to the different effects of scanning speed and hatching distance. Low scanning speed and hatching distance produced better tensile strength performance based on the fracture morphology in Figure 4.6(a). When the high scanning speed applied, improper melting will occur due to the insufficient energy delivered to the material and it has tendency to weaken the strength of the manufactured part. Also, when high hatching distance leads to insufficient overlapping between the layers and cause the powder particles to pack poorly. As a consequence, this has reduced the strength of the manufactured part.

4.2.4 Hardness

The resistance of a part when a force is applied can be determined via hardness tests. The obtained data can suggest the future performance of parts manufactured by SLM. Hardness depends on the stiffness, ductility, strain, plasticity, strength, viscosity and toughness of the manufactured part (Monroy, Delgado, Sereno, Ciurana, & Hendrichs, 2014).

The hardness values of the sixteen manufactured parts are tabulated in Table 4.11. ANOVA analysis was conducted to determine the most influential parameters on manufactured part hardness. Next, the larger-the-better approach and Equation (4.3) were used to calculate the S/N ratio and to find the optimum parameters for better hardness.

Table 4.11: Hardness and S/N ratio results

No	P, W	v, mm/s	h_d, mm	HV 1, HV	HV 2, HV	HV 3, HV	HV 4, HV	HV 5, HV	AVG HV, HV	S/N RATIO
1	120	250	0.08	214.00	230.00	235.00	264.00	257.00	240.00	47.60
2	120	510	0.1	264.00	248.00	246.00	258.00	253.00	253.80	48.09
3	120	760	0.12	273.00	276.00	275.00	277.00	266.00	273.40	48.74
4	120	900	0.14	271.00	272.00	279.00	265.00	272.00	271.80	48.68
5	200	250	0.1	262.00	263.00	268.00	269.00	256.00	263.60	48.42

Table 4.11, continued

6	200	510	0.08	258.00	264.00	278.00	277.00	278.00	271.00	48.66
7	200	760	0.14	288.00	273.00	271.00	279.00	271.00	276.40	48.83
8	200	900	0.12	285.00	287.00	281.00	289.00	283.00	285.00	49.10
9	275	250	0.12	266.00	258.00	254.00	253.00	265.00	259.20	48.27
10	275	510	0.14	257.00	248.00	252.00	252.00	266.00	255.00	48.13
11	275	760	0.08	246.00	247.00	243.00	250.00	247.00	246.60	47.84
12	275	900	0.1	236.00	236.00	235.00	238.00	235.00	236.00	47.46
13	360	250	0.14	205.00	215.00	218.00	211.00	215.00	212.80	46.56
14	360	510	0.12	227.00	235.00	233.00	234.00	234.00	232.60	47.33
15	360	760	0.1	260.00	252.00	245.00	250.00	241.00	249.60	47.94
16	360	900	0.08	245.00	254.00	250.00	246.00	244.00	247.80	47.88

The results were compared with a traditional process used for producing stainless steel 316L, which was 222 HV. According to the table above, the hardness of the manufactured parts was ranged from 212 – 285 HV. Based on the results, the parts manufactured by SLM were comparable to conventionally manufactured parts, whereby superior hardness values were obtained over conventional electron beam melting, casting and forging.

Table 4.11 indicates that the lowest hardness obtained was 212.80 HV at highest energy density of 10.28571429 J/mm^2. The melting with cracks phenomenon occurred on the manufactured part when higher energy input was applied, which involved greater laser power combined with a relatively low scanning speed. The manufactured part could be completely melted and even broken up due to the excessive shrinkage and high residual stresses that produced many visible cracks.

The ANOVA analysis for S/N ratios according to the larger-the-better principle is shown in Table 4.12 The p-values were compared to determine which parameter has the biggest impact on the hardness of manufactured parts. The data analysis indicates that laser power has the

greatest influence on hardness, because it had the lowest p-value (less than 0.05 significance level).

Table 4.12: ANOVA analysis for S/N ratios (hardness, R^2 = 80.31%)

Source	DF	Adj SS	Adj MS	F-Value	P-Value
P (W)	3	3156.9	1052.3	6.00	0.031
v (mm/s)	3	780.5	260.2	1.48	0.311
h_d (mm)	3	355.7	118.6	0.68	0.598
Error	6	1052.9	175.5	-	-
Total	15	5346.1	-	-	-

The average of each characteristic (S/N ratio) at each factor level is given in Table 4.13. Based on the S/N ratio results, laser power is the most influential on the hardness of manufactured parts, followed by scanning speed and then hatching distance.

Table 4.13: Response table for hardness

Level	Laser Power, W	Scanning speed, mm/s	Hatching distance, mm
1	48.28	47.71	48.00
2	48.75	48.05	47.98
3	47.93	48.34	48.36
4	47.43	48.28	48.05
Delta	1.32	0.62	0.38
Rank	1	2	3

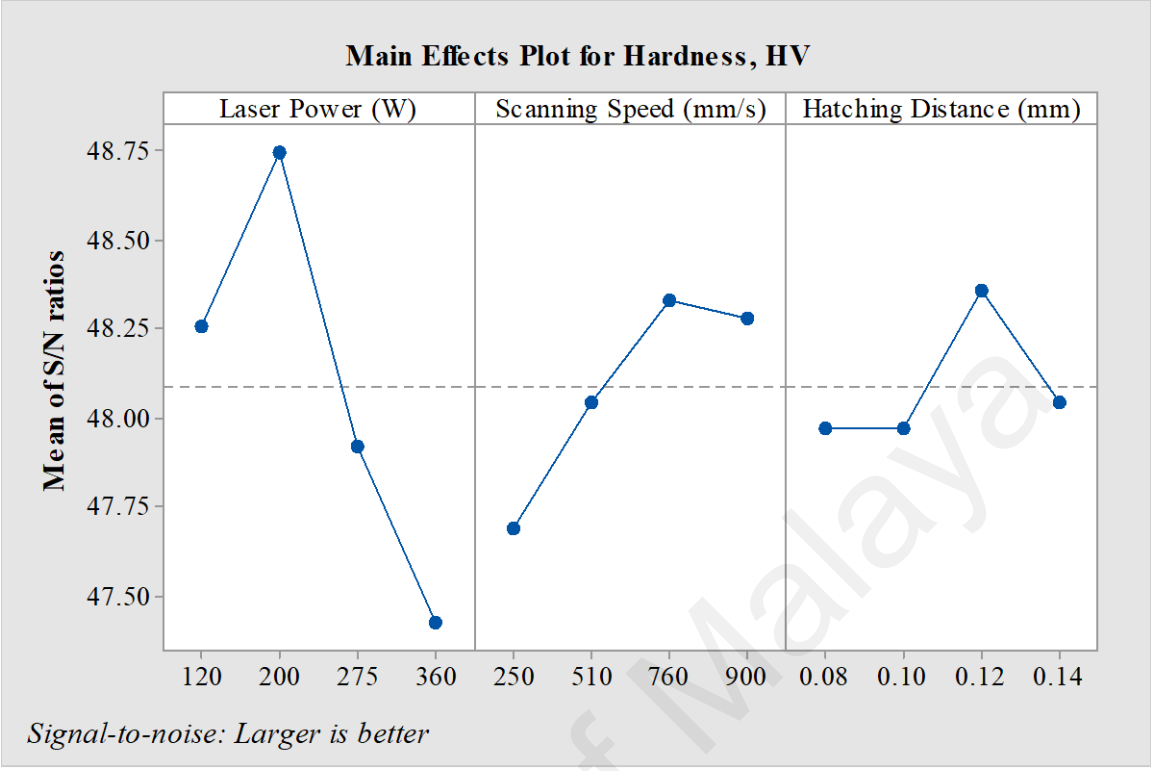

Figure 4.7: Main effects plot for hardness

As seen in Figure 4.7, the manufactured part hardness decreased rapidly when the laser power increased from 200 W to 360 W. This is because an excessive amount of liquid formed that reduced the viscosity of the manufactured part. The hardness also decreased when the lower scanning speed was applied. This is due to the higher energy density that leads to the widen of the melt pool area and the melt pool area is probably getting too hot. It leads to a too high cooling rate and the possible inclusion of gas bubbles. Hence, reduced the hardness of the manufactured part. The hardness of the manufactured parts increased when the hatching distance was 0.12 mm. Based on the Figure 4.7, when the hatching distance applied was less or more than 0.12 mm, the hardness of the manufactured parts decreased due to the detrimental effect that diminished the hardness of the manufactured part. However, when the high hatching distance was applied, the overlapping between the scan lines will be increased and lead to high porosity. As a result, the hardness of the manufactured part was reduced.

Therefore, the optimum parameters for good manufactured part having good hardness are at 200 W laser power, 760 mm/s scanning speed and 0.10 mm hatching distance.

4.2.5 Porosity

The density and porosity of the manufactured parts were measured using the volumetric method. The porosity percentages and S/N ratios of the manufactured parts are tabulated in Table 4.14.

Table 4.14: Porosity percentage and S/N ratio results

NO	P, W	v, mm/s	h_d, mm	Density (g/cm^3)	Porosity (%)	S/N Ratio
1	120	250	0.08	8.36	4.50	-13.07
2	120	510	0.1	7.49	6.32	-16.02
3	120	760	0.12	6.97	12.90	-22.21
4	120	900	0.14	6.55	18.17	-25.19
5	200	250	0.1	6.63	17.08	-24.65
6	200	510	0.08	8.29	3.66	-11.27
7	200	760	0.14	7.34	8.24	-18.32
8	200	900	0.12	7.23	9.63	-19.67
9	275	250	0.12	7.86	1.75	-4.86
10	275	510	0.14	6.61	17.34	-24.78
11	275	760	0.08	7.91	1.09	-0.76
12	275	900	0.1	8.31	3.89	-11.79
13	360	250	0.14	7.13	10.90	-20.75
14	360	510	0.12	7.85	1.82	-5.19
15	360	760	0.1	8.08	1.01	-0.06
16	360	900	0.08	8.43	5.38	-14.61

According to Table 4.14, the average density of manufactured parts was 7.57 g/cm^3. The ANOVA analysis for S/N ratios was done using the smaller-the-better approach with Equation (4.1) and the results are tabulated in Table 4.15. The p-values were compared to determine which parameter has the biggest impact on the strength of manufactured parts. Based on Table 4.15, the three factors do not have significant effects on the porosity of manufactured parts because the p-values were above the 0.05 significance level.

Table 4.15: ANOVA analysis for S/N ratios (Porosity percentage, R^2 = 70.47%)

Source	DF	Adj SS	Adj MS	F-Value	P-Value
P (W)	3	286.70	95.57	1.83	0.242
v (mm/s)	3	120.4	40.14	0.77	0.552
h_d (mm)	3	341.10	113.71	2.18	0.192
Error	6	313.6	52.26	-	-
Total	15	1061.8	-	-	-

The average of each characteristic (S/N ratio) for each factor level is given in Table 4.16. It seems that hatching distance has the greatest influence on the porosity of manufactured parts, followed by laser power and then scanning speed.

Table 4.16: Response table for porosity percentage, %

Level	Laser Power, W	Scanning Speed, mm/s	Hatching Distance, mm
1	-19.123	-15.832	-9.926
2	18.476	-14.314	-13.131
3	-10.547	-10.338	-12.983
4	-10.153	-17.816	-22.259
Delta	8.970	7.478	12.333
Rank	2	3	1

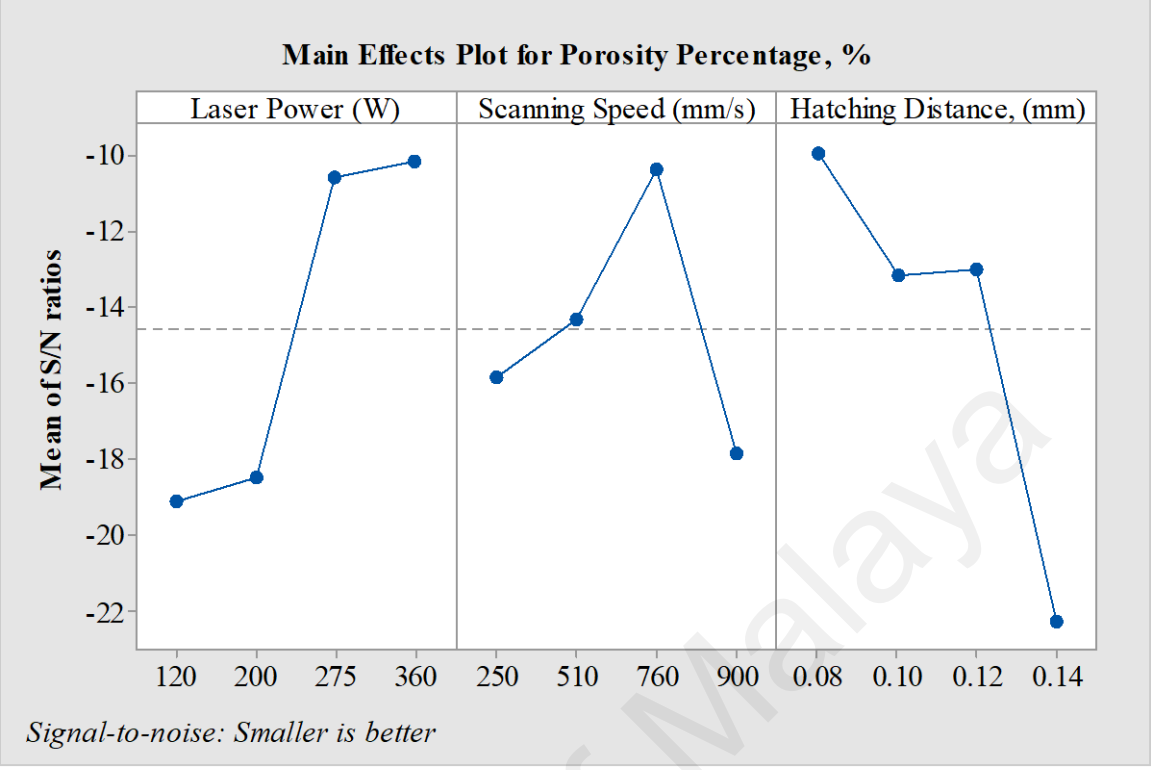

Figure 4.8: Main effects plot for porosity percentage, %

Based on Figure 4.8, the optimum parameters to obtain low porosity are 360 W laser power, 760 mm/s scanning speed and 0.08 mm hatching distance. Higher laser power produced the least porosity, as the laser input was sufficient to completely melt the stainless-steel powders. In contrast, low laser power produced higher porosity, as only limited liquid formed due to insufficient melting. The viscosity of the melt pool increases when a combination of un-melted balls and a liquid phase is present, which has a negative influence on the flowability of the liquid. Meanwhile, a low laser power beam may not be able to penetrate all the way to the previously solidified layer for the newly formed liquid to attach, resulting in poor wetting. Lower laser power may also mean less likelihood of powder ablation and plasma formation near the powder bed surface, thus lessening the overall "absorptivity" of the powder. A consequence of these various potential mechanisms is that large caves and crevices formed with many un-melted and half-melted particles within, as shown in Figure 4.9.

Less porosity was obtained at 760 mm/s scanning speed. The porosity percentage decreased between 250 mm/s and 760 mm/s. However, the porosity percentage decreased rapidly above 760 mm/s scanning speed because the laser scanning track exhibited discontinuity due to the balling phenomenon, as shown in Figure 4.9. The balling effect is possibly a consequence of an unstable melt pool; very high scanning speeds exert much more shear stress on the liquid phase, which generates higher surface tension inside the melt pool, leading to a high likelihood of ball formation. The splashing of liquid balls caused by very high scanning speeds also contributes to porosity under such processing conditions (Gu et al., 2013).

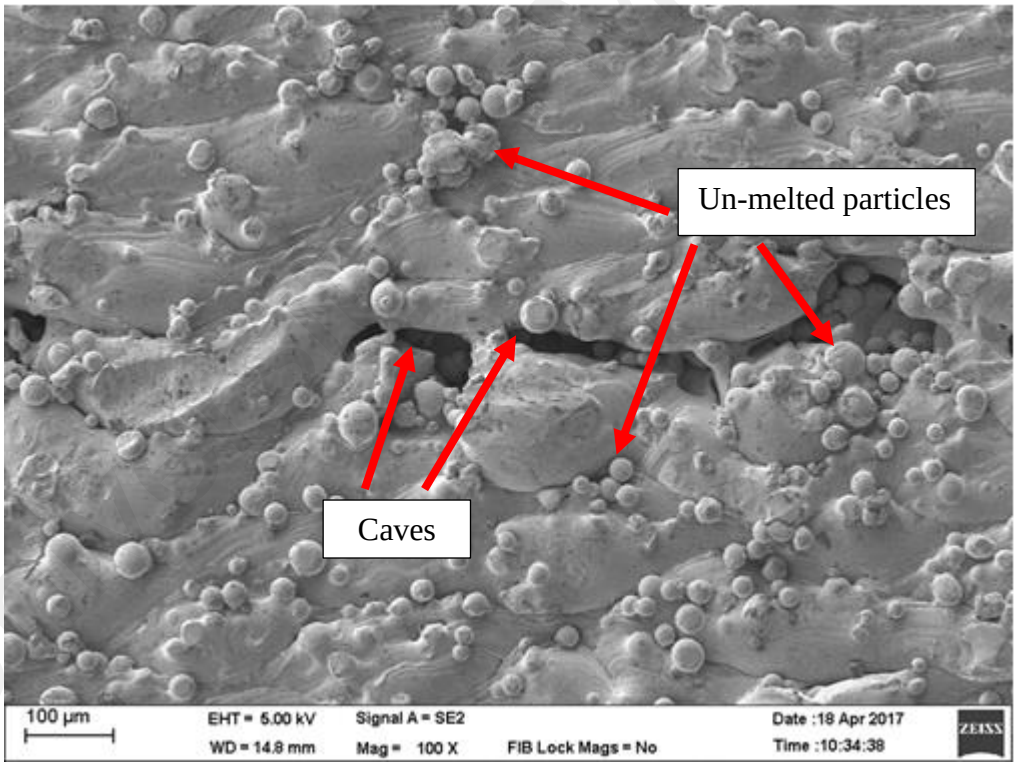

Figure 4.9: Metallographic observation: top view of 1st experiment

In addition, as shown in Figure 4.8, a short 0.08 mm hatching distance led to very low porosity percentage due to the greater overlap between melted zones. This means that the material lateral to the scan line, which melted previously (and was solidified), melted again.

It is suggested here that this phenomenon allows more of the trapped air to escape as bubbles. Furthermore, complete lateral melting is possible with shorter hatching distances, hence reducing the porosity.

4.3 Regression Analysis and Optimization

Further regression analysis was done to ensure the response values fit the model data. The regression analysis used in this work involved mathematical models to determine the relationship between the control parameters and performance of the manufactured parts based on the robust L_{16} orthogonal array design. The previous analysis yielded a response equation considering the effects of laser power (P), scanning speed (v) and hatching distance (h_d). The mathematical model produced relationships between the process parameters and output or response of this study as shown in the following equations.

4.3.1 Surface roughness

$$\text{Ra } [\mu m] = -3.27 + 0.06815\,(P) - 0.00845\,(v) + 77.5\,(h_d) \left[R^2 = 82.56\ \%\right] \quad (4.4)$$

Based on Equation (4.4), the predicted surface roughness value for the manufactured part obtained with the optimum parameters (120 W laser power, 900 mm/s scanning speed and 0.08 mm hatching distance) is 5.53 um.

4.3.2 Dimensional accuracy

$$\text{Accuracy } [\%] = -9.48 + 0.0795\,(P) - 0.00685\,(v) + 56.5\,(h_d) \left[R^2 = 60.01\ \%\right] \quad (4.5)$$

According to Equation (4.5), the predicted thickness value obtained for the manufactured part with the optimum parameters (120 W laser power, 200 mm/s scanning speed and 0.08 mm hatching distance) is 1.99 mm. Moreover, the dimensional error calculated is only 0.5%.

4.3.3 Tensile Strength

$$\text{Tensile Strength} = 659+0.569\ (P)-0.2613\ (v)-2142\ (h_d)\left[R^2=49.71\%\right] \quad (4.6)$$

According to Equation (4.6), the predicted tensile strength value obtained for the manufactured part based on the optimum parameters (275 W laser power, 250 mm/s scanning speed and 0.08 m,m hatching distance) is 603.58 MPa.

4.3.4 Hardness

$$\text{Hardness} = 256.5-0.1218\ (P)+0.0270\ (v)+99\ (h_d)\left[R^2=49.98\ \%\right] \quad (4.7)$$

The predicted hardness value obtained with Equation (4.7) for the optimum parameters (200 W laser power, 760 mm/s scanning speed and 0.12 mm hatching distance) is 288.73 HV.

4.3.5 Porosity

$$\text{Porosity}\ (\%) = -2.04-0.260\ (P)-0.00039\ (v)+147.3(h_d)\left[R^2=48.08\ \%\right] \quad (4.8)$$

The predicted porosity percentage obtained with Equation (4.8) for the optimum parameters (360 W laser power, 760 mm/s scanning speed and 0.08 mm hatching distance) is 1.22 %.

The optimum properties of the manufactured parts obtained from the S/N ratio graph are tabulated in Table 4.18, which also includes the values predicted by regression analysis.

4.4 Confirmation Experiment

A confirmation experiment was conducted using the optimal parameters obtained from the testing experiments and it has been compared with the predicted values from the regression analysis as in Table 4.17. The percentage error and accuracy of the predicted and experimental values were calculated with Equation (4.9) and (4.10).

$$\text{Percentage Error},\% = \left|\frac{k_0-k_1}{k_0}\right| \text{x } 100\% \quad (4.9)$$

$$\text{Accuracy, } A=\frac{1}{a}\Sigma_{i=1}^{a}\left(1-\frac{k_0-k_1}{k_0}\right)\text{x } 100\ \% \qquad (4.10)$$

Where k_0 is the predicted value, k_1 is the experimental value, , i=1, 2, 3 is the sample number and A is the accuracy of k sample data.

Table 4.17: Comparison between predicted and experimental values

Test	**Optimum parameters**			**Predicted value**	**Experimental value**	**Error (%)**	**Accuracy (%)**
	P, W	**v, mm/s**	**h_d, mm**				
Surface Roughness, Ra (um)	120	900	0.08	5.03	5.53	9.94	90.06
Thickness accuracy (mm)	120	900	0.08	1.99	2.03	2.01	97.90
Tensile Strength (MPa)	275	250	0.08	603.58	602.22	0.23	99.77
Hardness (HV)	200	760	0.10	288.73	292.8	1.41	98.61
Porosity (%)	360	760	0.08	1.22	0.99	18.85	81.15

The average percentage accuracy obtained is 93.50%. The low error level signifies that the results predicted by regression analysis are close to the actual experimental results. The error values indicate that the proposed model can predict the mechanical properties of manufactured parts satisfactorily.

4.4 Shot Peening

To complete the quality test analysis, shot peening was considered to investigate its effect on the quality of manufactured parts. Sample No. 6 was chosen for comparison.

Table 4.18: Value reductions after shot peening

Test	Before shot peening	After shot peening	Improvement (%)
Surface roughness, Ra (µm)	12.50	8.34	33.28
Dimensional accuracy (%)	6	2.5	58.33
Hardness (HV)	271	363.8	34.24

The values of the manufactured parts' mechanical properties before and after shot peening are provided in Table 4.18. The results indicate that the shot peening technique offered about 33.28% improvement in surface roughness, 58.33% improvement in dimensional accuracy and 34.24% improvement in hardness of the manufactured parts.

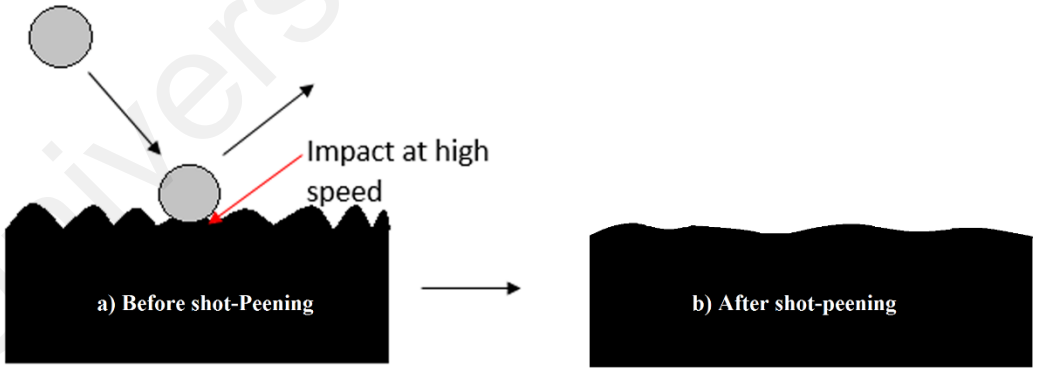

Figure 4.10: Illustration of the shot peening mechanism

This is a cold working process, whereby steel shots are decelerated onto the metal surface, thus enabling significant reductions in surface roughness (R_a) as illustrated in Figure 4.10 (Calignano et al., 2012).

a)

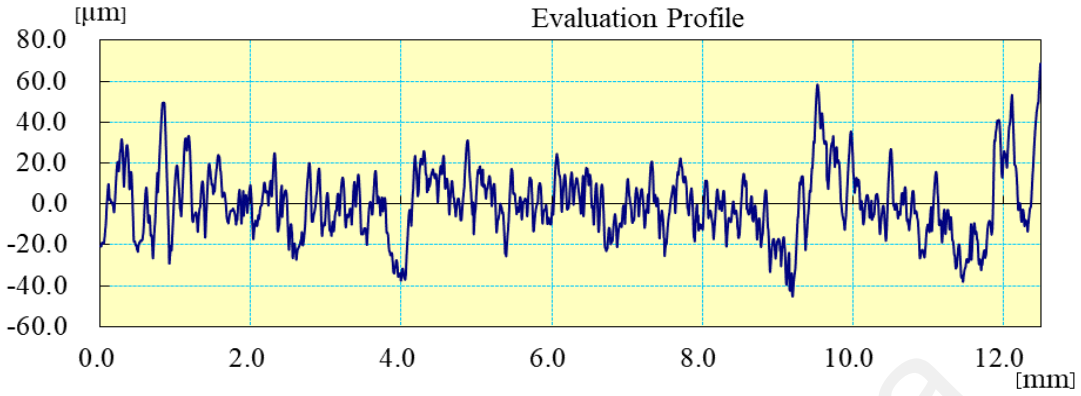

b)

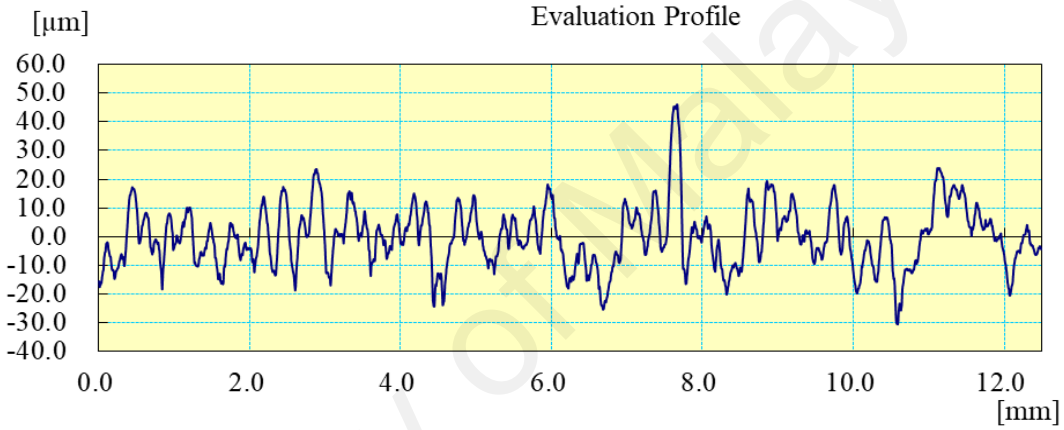

Figure 4.11: Sample 6: (a) before shot peening, (b) after shot peening

Figure 4.11 also clearly shows that the surface roughness of the produced parts was reduced greatly by shot peening, because the shot peening method involves high speed bombarded of the part surface with small spherical particles known as shots. Moreover, previous works have shown that shot peening, which involves a high velocity blast stream, produces fine dimples on the surface of the work material via impact erosions (Torres & Voorwald, 2002). This erosion process facilitates a smoother finishing on the parts without change in the dimensions nor contamination.

The surface roughness profile of the manufactured parts prior to and after the application of shot peening was captured using FESEM with 100x magnification. Figure 4.12 and 4.13 are images of the sample before and after shot peening. According to Figure 4.12 the spherical

balls (un-melted) of varying sizes appeared to be fused on the surface of the manufactured part, resulting in poor surface finish. After the shot peening process however, the surface of the manufactured part seemed free from un-melted spherical balls, indicating better surface finish as shown in Figure 4.13. This could be attributed to the removal of the un-melted spherical balls, burrs and imperfections in the part during shot peening. Thus, the shot peening process appears to facilitate significant improvement in the surface finish of SLM samples. According to the physical analysis in Figure 4.12 and 4.13, it can thus be concluded that shot peening also helps minimized the presence of necks or voids on the surface of manufactured parts.

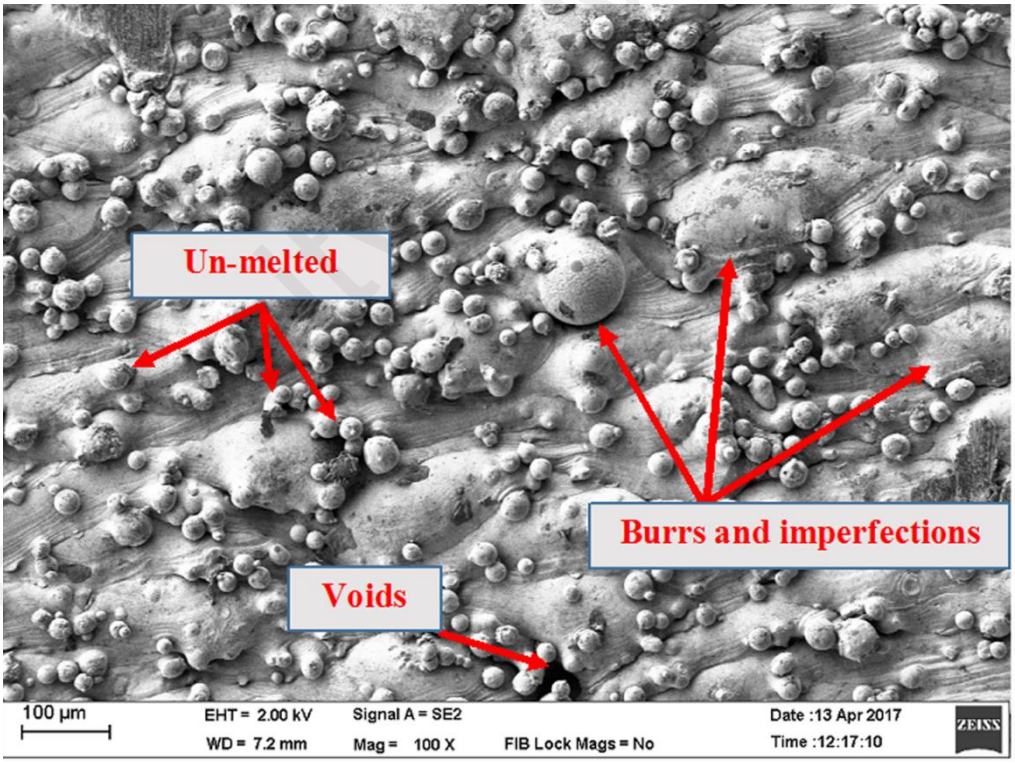

Figure 4.12: Micrograph images: Before shot peening

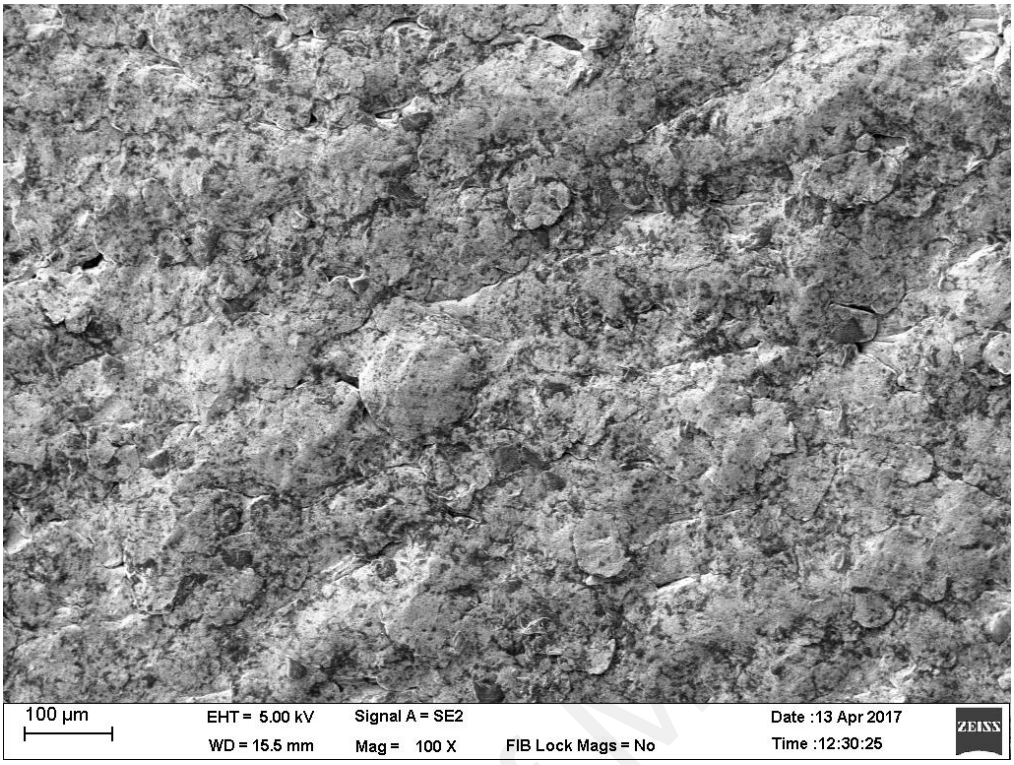

Figure 4.13:Micrograph images: After shot peening

CHAPTER 5 : CONCLUSION

5.1 Conclusion

The effect of process parameters on the mechanical properties of SS316L components produced using SLM was studied with the help of MINITAB® statistical software. The effects of three process parameters (i.e. laser power, hatching distance and scanning speed) on the surface roughness, dimensional accuracy, tensile strength, hardness and porosity of manufactured parts were investigated. According to analysis, laser power has the most significant effect on the surface roughness, dimensional accuracy, tensile strength and hardness of parts manufactured using the SLM technique. Moreover, data analysis indicated that hatching distance has the most significant effect on porosity percentage. The fracture morphology analysis demonstrated that the tensile strength is better when low scanning speed and hatching distance are applied.

In addition, the optimum parameters achieved at 120W of laser power, 900 mm/s of scanning speed and 0.08 mm of hatching distance for (surface roughness and dimensional accuracy), 275W of laser power, 250 mm/s of scanning speed and 0.08 mm of hatching distance for (tensile strength), 200 W of laser power, 760 mm/s of scanning speed and 0.10 mm of hatching distance for (hardness) and 360 W of laser power, 760 mm/s of scanning speed and 0.08 mm of hatching distance for (porosity percentage). Regression analysis was done on the predicted results compared with the confirmation test results according to the newly identified optimum parameters. Based on the comparison, the average accuracy is 93.50 %. Hence, the regression model can predict the mechanical properties of manufactured parts satisfactorily.

In addition, it was found that shot peening with steel shots helps enhance the quality of manufactured parts. The results indicate that shot peening facilitates improvements of about

33.28% for surface roughness, 58.33% for dimensional accuracy and 34.24% for hardness. The degree of improvement was affirmed with the FESEM images obtained and the physical appearance. The shot-peened samples appeared to possess higher surface integrity. Therefore, the shot peening post-processing technique is recommended for SLM components in other to obtain better overall surface quality.

5.2 Recommendations for future work

In this study, the effect of process parameters such as laser power, scanning speed and hatching distance on the physic-mechanical properties of the manufactured part have been investigated. Besides these three process parameters, the other influential parameters in SLM include building direction, layer thickness, laser source and laser beam size, which will significantly affect the physic-mechanical properties of the manufactured part. All of these parameters are not considered in this study. Therefore, the following works are recommended for future study:

- Investigate the effects of building direction, layer thickness, laser source and laser beam size on the physic-mechanical properties of the manufactured part.
- Parametric study in finite element model of SLM to evaluate the effects of the process parameters on the SLM process.

REFERENCES

Badrossamay, M., & Childs, T. (2006). Layer formation studies in selective laser melting of steel powders. *Proc. SFF Symp., Austin, Texas, USA*, 268-279.

Benardos, P. G., & Vosniakos, G. C. (2003). Predicting surface roughness in machining: a review. *International Journal of Machine Tools and Manufacture, 43*(8), 833-844.

Bin, H., & B, S. S. (2015). Curved Layer Adaptive Slicing (CLAS) for fused deposition modelling. *Rapid Prototyping Journal, 21*(4), 354-367.

Calignano, F., Manfredi, D., Ambrosio, E. P., Iuliano, L., & Fino, P. (2012). Influence of process parameters on surface roughness of aluminum parts produced by Direct Metal Laser Sintering. *The International Journal of Advanced Manufacturing Technology, 67*(9), 2743-2751.

Cherry, J. A., Davies, H. M., Mehmood, S., Lavery, N. P., Brown, S. G. R., & Sienz, J. (2015). Investigation into the effect of process parameters on microstructural and physical properties of 316L stainless steel parts by selective laser melting. *The International Journal of Advanced Manufacturing Technology, 76*(5), 869-879.

Chung, H., & Das, S. (2006). Processing and properties of glass bead particulate-filled functionally graded Nylon-11 composites produced by selective laser sintering. *Materials Science and Engineering: A, 437*(2), 226-234.

Delgado, J., Ciurana, J., & Rodríguez, C. A. (2011). Influence of process parameters on part quality and mechanical properties for Direct Metal Laser Sintering and Selective Laser Melting with iron-based materials. *The International Journal of Advanced Manufacturing Technology, 60*(5), 601-610.

Dewidar, M. M., Khalil, K. A., & Lim, J. K. (2007). Processing and mechanical properties of porous 316L stainless steel for biomedical applications. *Transactions of Nonferrous Metals Society of China, 17*(3), 468-473.

Frija, M., Hassine, T., Fathallah, R., Bouraoui, C., & Dogui, A. (2006). Finite element modelling of shot peening process: Prediction of the compressive residual stresses, the plastic deformations and the surface integrity. *Materials Science and Engineering: A, 426*(1–2), 173-180.

Gu, H., Gong, H., Pal, D., Rafi, K., Starr, T., & Stucker, B. (2013). Influences of energy density on porosity and microstructure of selective laser melted 17-4PH stainless steel. *2013 Solid Freeform Fabrication Symposium*, 474.

Guan, K., Wang, Z., Gao, M., Li, X., & Zeng, X. (2013). Effects of processing parameters on tensile properties of selective laser melted 304 stainless steel. *Materials & Design, 50*, 581-586.

Hanzl, P., Zetek, M., Bakša, T., & Kroupa, T. (2015). The Influence of Processing Parameters on the Mechanical Properties of SLM Parts. *Procedia Engineering, 100*, 1405-1413.

Ho, H., Cheung, W., & Gibson, I. (2002). Effects of graphite powder on the laser sintering behaviour of polycarbonate. *Rapid Prototyping Journal, 8*(4), 233-242.

Jugulum, R., & Samuel, P. (2008). Appendix D: Equations for Signal-to-Noise (S/N) Ratios *Design for Lean Six Sigma* (pp. 277-280): John Wiley & Sons, Inc.

Kamarudin, K., Wahab, M., Raus, A., Ahmed, A., & Shamsudin, S. (2017). *Benchmarking of dimensional accuracy and surface roughness for AlSi10Mg part by selective laser melting (SLM).* Paper presented at the AIP Conference Proceedings.

Kearns, M., & Murray, K. (2010). Gas atomised powders cut energy costs. *Metal Powder Report, 65*(3), 16-20.

Kempen, K., Thijs, L., Van Humbeeck, J., & Kruth, J. P. (2012). Mechanical Properties of AlSi10Mg Produced by Selective Laser Melting. *Physics Procedia, 39*(Supplement C), 439-446.

Krakhmalev, P., Fredriksson, G., Yadroitsava, I., Kazantseva, N., Plessis, A. d., & Yadroitsev, I. (2016). Deformation Behavior and Microstructure of Ti6Al4V Manufactured by SLM. *Physics Procedia, 83*, 778-788.

Krishnan, M., Atzeni, E., Canali, R., Calignano, F., Manfredi, D., Ambrosio, E. P., & Iuliano, L. (2014). On the effect of process parameters on properties of Aluminium (AlSi10Mg) parts produced by Direct Metal Laser Sintering. *Rapid Prototyping Journal, 20*(6), 449-458.

Kruth, J.-P., Badrossamay, M., Yasa, E., Deckers, J., Thijs, L., & Van Humbeeck, J. (2010). *Part and material properties in selective laser melting of metals.* Paper presented at the Proceedings of the 16th international symposium on electromachining.

Lee, P.-H., Chung, H., Lee, S. W., Yoo, J., & Ko, J. (2014). Review: Dimensional Accuracy in Additive Manufacturing Processes. (45806), V001T004A045.

Makoana, N. W., Möller, H., Burger, H., Tlotleng, M., & Yadroitsev, I. (2016). *Evaluation of single tracks of 17-4PH steel manufactured at different power densities and scanning speeds by selective laser melting* (Vol. 27).

Monroy, K. P., Delgado, J., Sereno, L., Ciurana, J., & Hendrichs, N. J. (2014). Effects of the Selective Laser Melting manufacturing process on the properties of CoCrMo single tracks. *Metals and Materials International, 20*(5), 873-884.

Negi, S., Dhiman, S., & Sharma, R. K. (2015). Influence of Process Parameters on Mechanical Properties of Parts Fabricated by Selective Laser Sintering.

Phadke, M. S. (1995). *Quality engineering using robust design*: Prentice Hall PTR.

Rahmati, B., Sarhan, A. A. D., & Sayuti, M. (2014). Investigating the optimum molybdenum disulfide (MoS2) nanolubrication parameters in CNC milling of AL6061-T6 alloy. *The International Journal of Advanced Manufacturing Technology, 70*(5), 1143-1155. doi:10.1007/s00170-013-5334-x

Sateesh, N. H., Kumar, G. C. M., Prasad, K., C.K, S., & Vinod, A. R. (2014). Microstructure and Mechanical Characterization of Laser Sintered Inconel-625 Superalloy. *Procedia Materials Science, 5*, 772-779.

Sharma, V. S., Singh, S., Sachdeva, A., & Kumar, P. (2013). Influence of sintering parameters on dynamic mechanical properties of selective laser sintered parts. *International Journal of Material Forming, 8*(1), 157-166.

Simchi, A. (2006). Direct laser sintering of metal powders: Mechanism, kinetics and microstructural features. *Materials Science and Engineering: A, 428*(1), 148-158.

Simchi, A., & Pohl, H. (2003). Effects of laser sintering processing parameters on the microstructure and densification of iron powder. *Materials Science and Engineering: A, 359*(1–2), 119-128.

Song, B., Dong, S., Deng, S., Liao, H., & Coddet, C. (2014). *Microstructure and tensile properties of iron parts fabricated by selective laser melting* (Vol. 56).

Song, Y.-A., & Koenig, W. (1997). Experimental Study of the Basic Process Mechanism for Direct Selective Laser Sintering of LowMelting Metallic Powder. *Cirp Annals-manufacturing Technology, 46*(1), 127-130.

Stucker, B. (2001). *The selective laser sintering process*. Magnolia: Magnolia Publishing inc.

Stwora, A., & Skrabalak, G. (2013). Influence of selected parameters of Selective Laser Sintering process on properties of sintered materials. *Journal of achievements in materials and manufacturing engineering, 61*(2), 375-380.

Tolosa, I., Garciandía, F., Zubiri, F., Zapirain, F., & Esnaola, A. (2010). Study of mechanical properties of AISI 316 stainless steel processed by "selective laser melting", following different manufacturing strategies. *The International Journal of Advanced Manufacturing Technology, 51*(5-8), 639-647.

Torres, M. A. S., & Voorwald, H. J. C. (2002). An evaluation of shot peening, residual stress and stress relaxation on the fatigue life of AISI 4340 steel. *International Journal of Fatigue, 24*(8), 877-886.

Yap, C., Chua, C., Dong, Z., Liu, Z., Zhang, D., Loh, L., & Sing, S. (2015). Review of selective laser melting: Materials and applications. *Applied physics reviews, 2*(4), 041101.

Zhang, B., Liao, H., & Coddet, C. (2012). *Effects of processing parameters on properties of selective laser melting Mg–9%Al powder mixture* (Vol. 34).

SUPPLEMENTARY

LIST OF PUBLICATION AND PAPER PRESENTED

1. "Effects of Process Parameters on Surface Roughness of Stainless Steel 316L Parts Produced by Selective Laser Melting", Journal of testing and evaluation - Accepted
2. "Effects of Process Parameters on Surface Roughness of Stainless Steel 316L Parts Produced by Selective Laser Melting" 2017 2nd Advanced Research in Engineering and Information Technology International Conference- Paper Presented